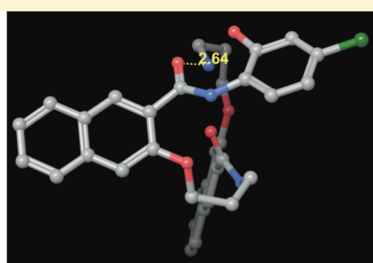


Identification of a Potent Inhibitor of CREB-Mediated Gene Transcription with Efficacious in Vivo Anticancer Activity

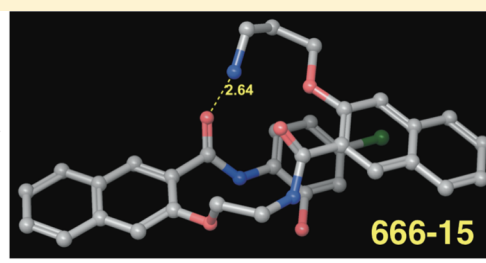
Fuchun Xie,^{†,||} Bingbing X. Li,^{†,||} Alina Kassenbrock,[†] Changhui Xue,[‡] Xiaoyan Wang,[§] David Z. Qian,[‡] Rosalie C. Sears,^{§,‡} and Xiangshu Xiao^{*,†,‡}

[†]Program in Chemical Biology, Department of Physiology and Pharmacology, [‡]Knight Cancer Institute, and [§]Department of Medical and Molecular Genetics, Oregon Health & Science University, 3181 SW Sam Jackson Park Road, Portland, Oregon 97239, United States

Supporting Information



CREB inhibitor ($IC_{50} = 2220 \text{ nM}$)



CREB inhibitor ($IC_{50} = 81 \text{ nM}$)

ABSTRACT: Recent studies have shown that nuclear transcription factor cyclic adenosine monophosphate response element binding protein (CREB) is overexpressed in many different types of cancers. Therefore, CREB has been pursued as a novel cancer therapeutic target. Naphthol AS-E and its closely related derivatives have been shown to inhibit CREB-mediated gene transcription and cancer cell growth. Previously, we identified naphthamide **3a** as a different chemotype to inhibit CREB's transcription activity. In a continuing effort to discover more potent CREB inhibitors, a series of structural congeners of **3a** was designed and synthesized. Biological evaluations of these compounds uncovered compound **3i** (**666-15**) as a potent and selective inhibitor of CREB-mediated gene transcription ($IC_{50} = 0.081 \pm 0.04 \mu\text{M}$). **666-15** also potently inhibited cancer cell growth without harming normal cells. In an in vivo MDA-MB-468 xenograft model, **666-15** completely suppressed the tumor growth without overt toxicity. These results further support the potential of CREB as a valuable cancer drug target.

INTRODUCTION

The cAMP-response element binding protein (CREB) is a nuclear transcription factor that can be activated to initiate gene transcription in response to hormones, growth factors, and neuronal activity.^{1,2} These stimuli activate intracellular protein serine/threonine kinases such as mitogen-activated protein kinase (MAPK), protein kinase A (PKA), protein kinase B (PKB/Akt), and p90 ribosomal S6 kinase (p90^{RSK}).³ All these kinases have been shown to be able to phosphorylate Ser133 in CREB.^{1,3} Phosphorylation at Ser133 is crucial in CREB's binding with histone acetyl transferase and mammalian transcription coactivator CREB-binding protein (CBP) and its paralog p300 to initiate CREB-dependent gene transcription. The binding interaction between CREB and CBP/p300 is mediated by the activation domain in CREB called kinase-inducible domain (KID) and KID-interacting (KIX) domain in CBP/p300.⁴ Three protein phosphatases, protein phosphatase 1 (PP1),⁵ protein phosphatase 2A (PP2A),⁶ and phosphatase and tensin homolog (PTEN),⁷ have been shown to dephosphorylate Ser133 in phosphorylated CREB to turn off CREB-dependent gene transcription.

The protein kinases leading to CREB activation are frequently overactivated, while the three phosphatases to dephosphorylate CREB are often inactivated in various cancer cells. Therefore, it was predicted that CREB would be overactivated in cancer cells. Consistent with this prediction, CREB and phosphorylated CREB have been consistently shown to be overexpressed in cancer tissues from brain,^{8,9} breast,^{10,11} lung,¹² prostate,¹³ and bone marrow.¹⁴ Because of its aberrant activation in cancer cells, CREB has been pursued as a novel cancer therapeutic target.³ We recently identified naphthol AS-E (**1**, Figure 1) as a cell-permeable inhibitor of CREB-mediated gene transcription through inhibiting KID-KIX interaction,¹⁵ the essential protein–protein interaction to activate CREB-dependent gene transcription.⁴ Consistent with the important roles of CREB in the maintenance of cancer cells, we found that **1** and its close related derivatives selectively inhibited proliferation of a large panel of cancer cell lines from different organs in the low micromolar concentration range without harming normal cells in vitro.¹⁶

Received: March 22, 2015

Published: May 29, 2015

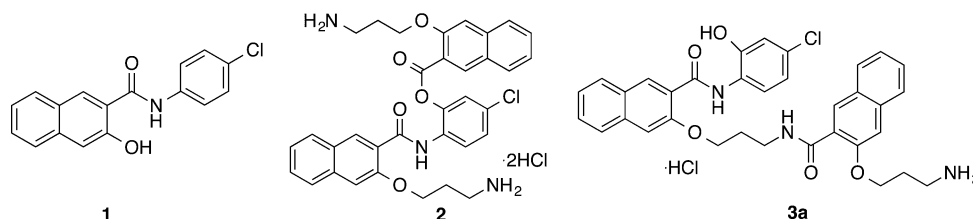


Figure 1. Chemical structures of previously reported CREB inhibitors: naphthol AS-E (**1**) and compounds **2** and **3a**. Compound **2** is rapidly transformed into **3a** through an *O,N*-acyl transfer reaction at pH 7.4.

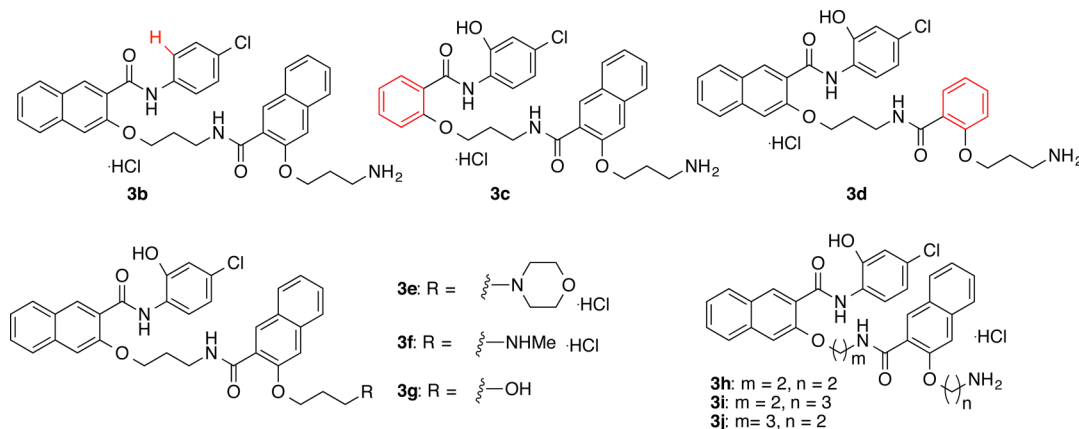


Figure 2. Chemical structures of newly designed structural congeners (**3b–j**) of **3a**. The key structural difference between **3b–d** and **3a** is highlighted in red.

During our course of studies to improve the aqueous solubility and biological activity of **1**, we designed and synthesized compound **2** (Figure 1). Compound **2** presented significantly improved antiproliferative activity against a panel of different cancer cells.¹⁷ Unexpectedly, we found that **2** was rapidly converted into **3a** under physiological conditions and was considered as a prodrug of **3a**, where a long-range *O,N*-acyl transfer reaction was involved (Figure 1).¹⁷ While **2** displayed in vivo antitumor cancer activity, its CREB inhibition potency remained modest.¹⁷ In this report, we detail our optimization of **3a** and identification of **3i** (**666-15**) as a potent CREB inhibitor with highly efficacious in vivo antitumor cancer activity.

RESULTS AND DISCUSSION

Analog Design Rationale. A series of structural congeners of **3a** shown in Figure 2 was designed to improve its biological activities and physicochemical properties. Compound **3a** contains a phenolic hydroxyl group that is a potential site for glucuronidation, which would limit its metabolic stability and bioavailability.^{18–20} To test if this potential metabolic liability can be removed without compromising bioactivity, compound **3b** was designed to interrogate the role of the phenol group in **3a** in contributing to its bioactivity. Compound **3a** also has relatively high polar surface area (PSA, 123.2 Å²) and high cLogP (5.30) (Table 1). To improve these two physicochemical parameters, compounds **3c,d** were designed by removing one of the conjugated planar naphthyl rings. Truncating one of the naphthyl ring systems into a benzene system decreases the PSA to ~98 Å² and cLogP to ~4.9 (Table 1). Compounds **3e–g** were designed to probe the role of the primary amino group in **3a**. If this primary amino group tolerates structural changes, additional functional groups may be attached to the primary amino group. Analogs **3h–j** were designed by varying the lengths of the linker and side chain to understand their roles in

Table 1. Physicochemical Properties and CREB Inhibition Activity of 3a–j

compd	PSA ^a (Å ²)	cLogP ^a	CREB inhibition IC ₅₀ (μM) ^b
3a	123.2	5.30	2.22 ± 0.38
3b	86.9	6.41	4.69 ± 1.28
3c	98.0	4.91	10.05 ± 2.29
3d	97.9	4.92	5.30 ± 1.41
3e	96.1	5.42	>50
3f	92.45	5.87	18.53 ± 8.68
3g	105.8	5.26	7.30 ± 1.66
3h	100.2	4.43	0.30 ± 0.12
3i	100.2	4.83	0.081 ± 0.04
3j	100.0	5.39	5.23 ± 0.36

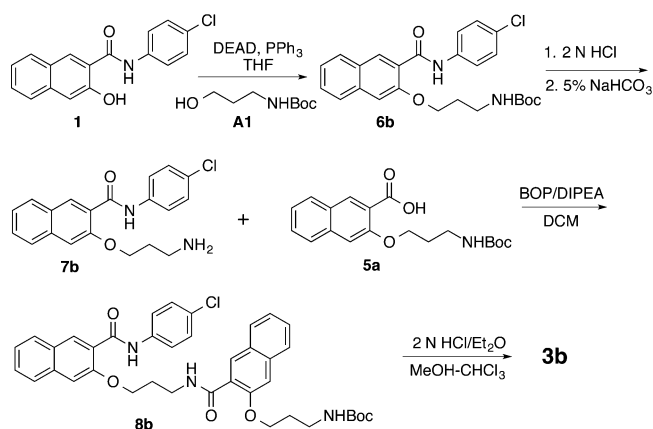
^aThe polar surface area (PSA) and calculated log *P* (cLogP) values were computed from their global energy minima using QikProp.

^bCREB inhibition refers to inhibition of CREB-mediated gene transcription in HEK 293T cells using a CREB reporter assay. The IC₅₀ was presented as the mean ± SD of at least two independent experiments in triplicate or >50 in the cases where the IC₅₀ was not reached at the highest tested concentration (50 μM).

biological activities. As presented in Table 1, compounds **3e–j** show decreased PSA and **3g–i** also present decreased cLogP compared to **3a**.

Chemistry. The synthesis of compounds **3b–j** is presented in Schemes 1–7 and is overall similar to the synthesis of **3a** as described before.¹⁷ All the final products were prepared in good to excellent yields. This synthesis of **3b** is shown in Scheme 1. Mitsunobu coupling (Ph₃P/DEAD)²¹ between **1** and Boc-protected 3-amino-1-propanol (**A1**) gave **6b**, whose Boc protecting group was removed under acidic condition to generate free base **7b** after neutralization with NaHCO₃. Amide formation between amine **7b** and previously reported acid **5a**¹⁷ under the BOP/DIPEA coupling condition yielded amide **8b**.

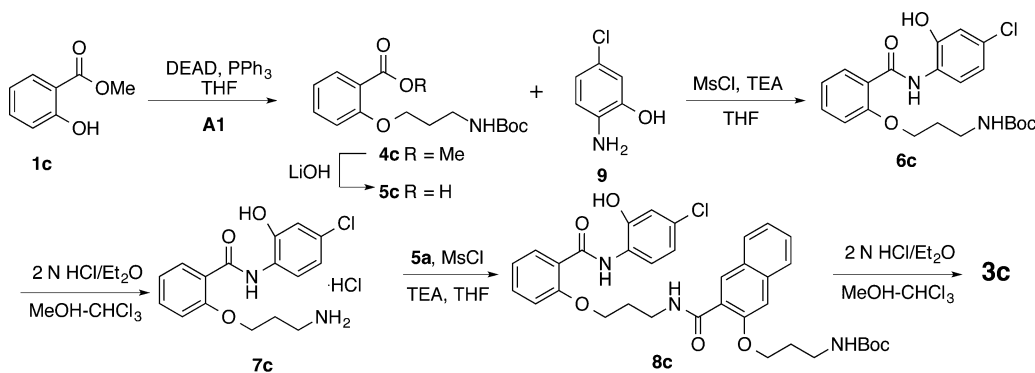
Scheme 1. Synthesis of Compound 3b



Deprotection of Boc in **8b** with 2 N HCl delivered product **3b**. Compound **3c** was prepared in a similar fashion with the exception of a need for **7c** as the key intermediate (Scheme 2). The commercially available starting materials methyl salicylate (**1c**) and **A1** were coupled together under Mitsunobu reaction condition. Saponification of methyl ester **4c** generated acid **5c**, which was then coupled with aniline **9** to yield **6c** with MsCl as the activating reagent.²² The activating reagent MsCl was found to be superior to BOP in achieving high selectivity for forming desired amide versus the alternative undesired ester.¹⁷ Removal of the Boc group from **6c** provided amine **7c**, which was further coupled with acid **5a** followed by acidic deprotection of Boc to give desired product **3c**. The activating reagent MsCl was again found to be superior to BOP in achieving high selectivity for forming desired amide versus the alternative ester and was selected for all the subsequent amide formation reactions. Compound **3d** was prepared in two steps by coupling between amine **7a**¹⁷ and acid **5c** followed by Boc deprotection (Scheme 3).

The preparation of morpholine substituted compound **3e** is shown in Scheme 4. The morpholine side chain was incorporated into **1a**²³ by Mitsunobu reaction with **A2**. Saponification of ester **4e** provided acid **5e**, which was then coupled with amine **7a** by MsCl/Et₃N to afford amide **8e**. Treatment of **8e** with HCl yielded corresponding hydrochloride salt **3e**. A similar sequence of reactions was employed to prepare **3f** and **3g**. The side chain in **4g** was installed by O-alkylation of naphthol **1a**, while the *N*-methyl group in **4f** was introduced by methylation of carbamate **4a** by NaH/MeI.²⁴

Scheme 2. Synthesis of Compound 3c

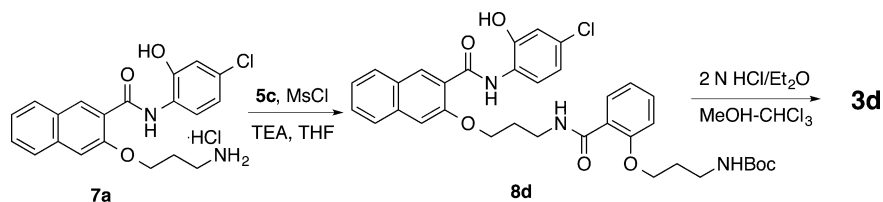


Compounds **3h–j** having different linker and side chain lengths were synthesized as shown in Schemes 5–7. Intermediate **7h** was prepared essentially the same as that for **7a**¹⁷ with the use of **A4** as the Mitsunobu coupling partner followed by saponification, amide formation, and Boc deprotection. Amide coupling between the amine **7h** and acid **5h** generated amide **8h**, whose Boc was removed under acidic condition to provide **3h**. Intermediates **8i** and **8j** were prepared by assembling building blocks **5a** and **7h**, **5h** and **7a**, respectively (Schemes 6 and 7). Final deprotection of Boc in **8i** and **8j** delivered desired compounds **3i** and **3j** uneventfully.

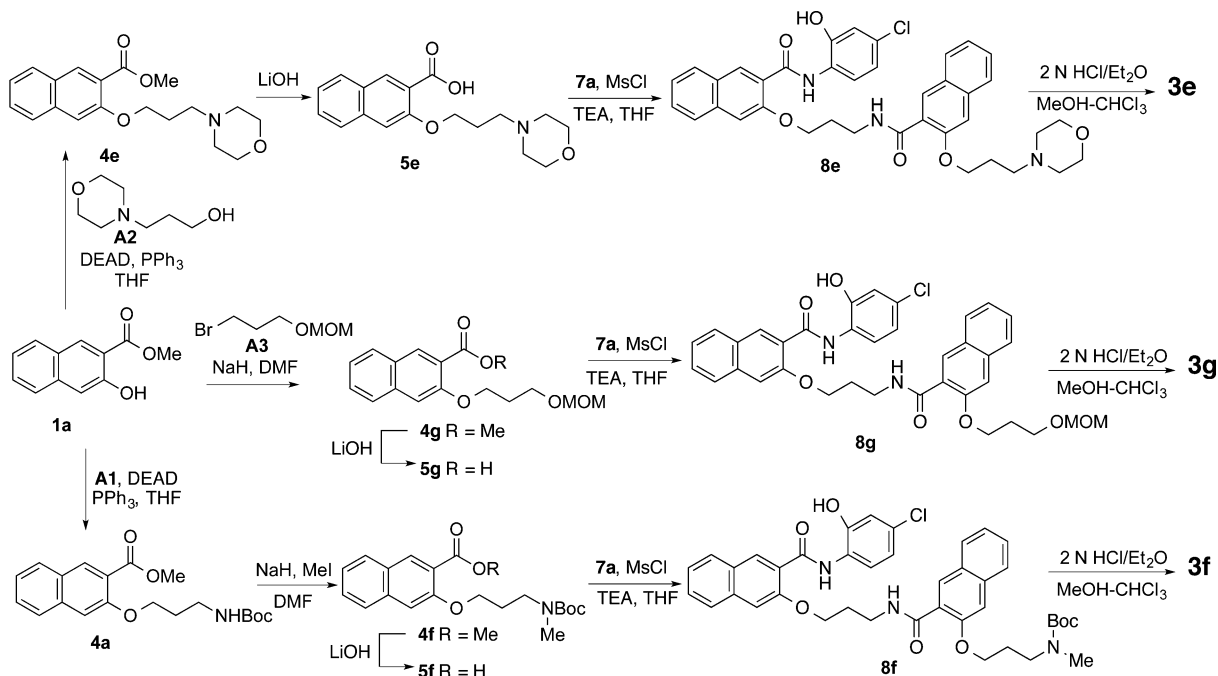
Inhibition of CREB-Mediated Gene Transcription by 3b–j. The newly synthesized final compounds **3b–j** were evaluated for their activity in inhibiting CREB-mediated gene transcription in HEK 293T cells using a CREB *Renilla* luciferase (RLuc) reporter assay.¹⁵ In this assay, HEK 293T cells were transfected with a RLuc reporter under the control of a synthetic CREB promoter containing three copies of cAMP-response elements (CRE). The transfected cells were then treated with different concentrations of compounds for 30 min before the induction of RLuc synthesis by forskolin (10 μM), an activator of adenylate cyclase to activate CREB's transcription activity.²⁵ The results from this CREB reporter assay are summarized in Table 1, where the concentrations required to inhibit 50% of CREB's transcription activity (IC₅₀) are shown. For comparison purpose, the potency of previously reported compound **3a** (IC₅₀ = 2.22 μM) was also included in Table 1.¹⁷

In comparison to **3a**, compound **3b** without the phenol group showed about 2-fold decrease of activity in CREB inhibition (IC₅₀ = 4.69 μM), indicating that the phenol group in **3a** has a beneficial effect on CREB inhibition. Therefore, the rest of the compounds were designed to retain this crucial phenol group. Compounds **3c** and **3d**, with one of the naphthyl rings being trimmed down to a benzene ring, displayed approximately 2- to 5-fold less potent CREB inhibition activity than **3a**, suggesting that the two naphthyl rings could not be simplified to phenyl rings without compromising CREB inhibitory activity. Replacement of the primary amino group in **3a** with morpholine (**3e**), *N*-methlamino (**3f**), or hydroxyl (**3g**) group resulted in a total loss of CREB inhibition activity for **3e** (IC₅₀ > 50 μM) and significant decrease in CREB inhibition activity for **3f** (IC₅₀ = 18.53 μM) and **3g** (IC₅₀ = 7.30 μM). These data indicated that the primary amino group at the side chain of **3a** is critical for maintaining CREB inhibition activity and not suitable for even minor modifications like methylation.

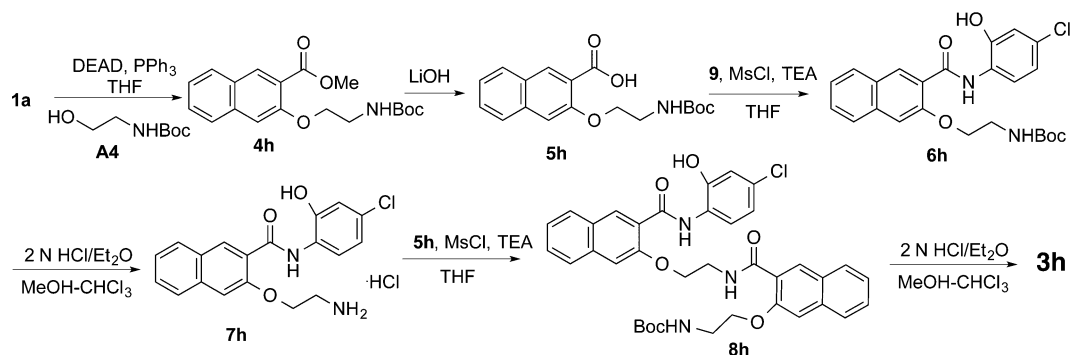
Scheme 3. Synthesis of Compound 3d



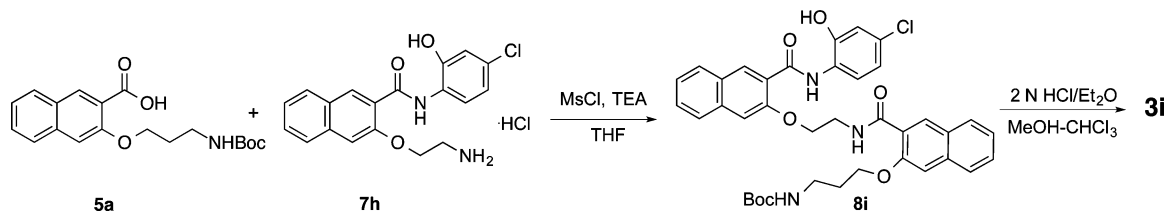
Scheme 4. Synthesis of Compounds 3e–g



Scheme 5. Synthesis of Compound 3h



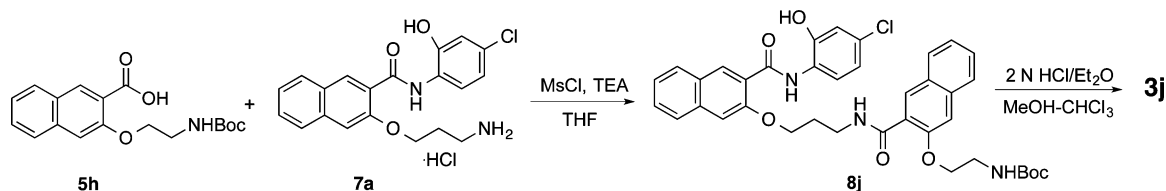
Scheme 6. Synthesis of Compound 3i



We then focused on the modification of the lengths of the linker between the two naphthyl rings and the side chain in compound 3a to interrogate their roles in CREB inhibition activity. Specifically, compounds 3h–j with two- or three-

carbon chains were designed and synthesized. Gratifyingly, compound 3h with a two-carbon linker and a two-carbon side chain showed significantly increased CREB inhibition activity (IC₅₀ = 0.30 μM) compared to 3a. Furthermore, compound 3i

Scheme 7. Synthesis of Compound 3j

Table 2. Antiproliferative Activities of 3a–j^a

compd	GI ₅₀ (μM)			
	A549	MCF-7	MDA-MB-231	MDA-MB-468
3a	0.29 ± 0.01	0.14 ± 0.03	0.37 ± 0.13	0.22 ± 0.07
3b	0.95 ± 0.77	1.72	1.00 ± 0.58	1.62 ± 0.48
3c	2.44 ± 0.40	2.30 ± 0.67	4.61 ± 2.20	1.82 ± 0.20
3d	2.32 ± 0.35	2.66 ± 1.30	5.82 ± 4.61	2.32 ± 0.39
3e	>100	>100	>100	13.74 ± 3.98
3f	0.26 ± 0.06	1.65 ± 0.44	0.26 ± 0.04	0.20 ± 0.02
3g	39.15 ± 32.09	28.99 ± 10.27	82.67 ± 24.52	10.19 ± 1.47
3h	1.16 ± 0.05	0.81 ± 0.78	1.21 ± 0.15	0.25 ± 0.01
3i	0.47 ± 0.06	0.31 ± 0.10	0.073 ± 0.04	0.046 ± 0.04
3j	2.17 ± 0.11	1.89 ± 0.60	2.71 ± 0.32	1.85 ± 0.23

^aGI₅₀ is the concentration required to inhibit the cancer cell growth by 50% as evaluated by the MTT assay. The compounds were incubated with cells for 72 h. The GI₅₀ was presented as mean ± SD of at least two independent experiments in duplicates or >100 in the cases where GI₅₀ was not reached at the highest tested concentration (100 μM). When SD was not presented, only one experiment was performed in duplicate.

with a two-carbon linker and a three-carbon side chain exhibited even more potent CREB inhibition activity (IC₅₀ = 81 nM), which is approximately 28-fold improvement over 3a. The enhancement of CREB inhibition activity seen for 3i is very structure-specific because its structural isomer 3j, which has a three-carbon linker and two-carbon side chain, was a much weaker CREB inhibitor with an IC₅₀ of 5.23 μM. The CREB inhibitory potency difference among 3a and 3h–j demonstrated that the length of the linker between the two naphthyl rings can dramatically affect the activity and the length of the side chain also has a critical role on the CREB inhibition activity.

Inhibition of Cancer Cell Proliferation by 3b–j. We also evaluated the antiproliferative activity of compounds 3b–j in four different cancer cell lines: A549 (non-small-cell lung cancer), MCF-7 (breast cancer), MDA-MB-231 (breast cancer), and MDA-MB-468 (breast cancer) using the colorimetric MTT [3-(4,5-dimethylthiazol-2-yl)-2,5-diphenyltetrazolium bromide] assay.^{16,26} The concentrations required to inhibit 50% of the cancer cell growth (GI₅₀) are presented in Table 2. As reported before,¹⁷ compound 3a was a submicromolar inhibitor of proliferation of all the four cancer cell lines tested. The analogs 3b–e all presented less potent antiproliferative activity than 3a, in agreement with their reduced CREB inhibition potency. Although 3e was inactive in the CREB reporter assay, it showed weak growth inhibition activity in MDA-MB-468 cells (GI₅₀ = 13.74 μM) but no activity in the other three cancer cell lines. It is unlikely that the weak activity in MDA-MB-468 cells was a result of inhibition of CREB's transcription activity. Similar discrepancy was also observed for 3f, which exhibited weak CREB inhibition activity while displaying robust antiproliferative activity in these four cancer cell lines. The GI₅₀ for 3f is 0.26, 1.65, 0.26, and 0.20 μM in A549, MCF-7, MDA-MB-231, and MDA-MB-468 cells, respectively. Compound 3g displayed modest CREB inhibition activity, but it was a rather weak inhibitor of proliferation in all

four cancer cell lines tested with GI₅₀ values ranging from 10.19 to 82.67 μM. Finally, in the series of compounds 3h–j with different lengths of the linker and side chain, we observed that potent CREB inhibitor 3i also potently inhibited cancer cell growth. In MDA-MB-231 and MDA-MB-468 cells, the GI₅₀ for 3i was 73 and 46 nM, respectively. In A549 and MCF-7 cells, it exhibited robust activity as well with GI₅₀ of 0.47 and 0.31 μM. Compared to 3i, 3h retained reasonable CREB inhibition activity and inhibition of cancer cell growth while 3j was much less potent. Therefore, compound 3i represents the most potent CREB inhibitor bearing potent anticancer activity reported to date.^{15–17,27,28}

Previously, it was shown that 3a only weakly inhibited CREB-CBP interaction (IC₅₀ = 19.72 ± 1.78 μM) as assayed by a split RLuc complementation assay.¹⁷ We also investigated if the more potent CREB inhibitor 3i could inhibit CREB-CBP interaction using the same assay. It was also found to be a rather weak inhibitor of CREB-CBP interaction with IC₅₀ = 18.27 ± 2.81 μM. We conclude that 3i inhibits CREB's transcription activity in living cells independent of direct CREB or CBP binding interaction. Further studies are needed to understand if 3i will modulate the upstream components of CREB activation.³ Or alternatively, an unbiased chemo-proteomics approach²⁹ may be utilized to identify the direct target of 3i to understand its mechanism of inhibiting CREB-mediated gene transcription.

The results presented above showed that the bioactivities of 3a are very sensitive to structural modifications to either increase or decrease its activity. The physicochemical property parameters like PSA³⁰ and cLogP³¹ that are associated with cell membrane permeability do not seem to be the major determinants. For example, compounds 3h–j bear similar PSA, but their bioactivities do not correlate with their cLogP (Table 1). To identify the structural basis for the observed bioactivity differences among 3a and 3h–j, we performed conformational searches to identify their global conformational

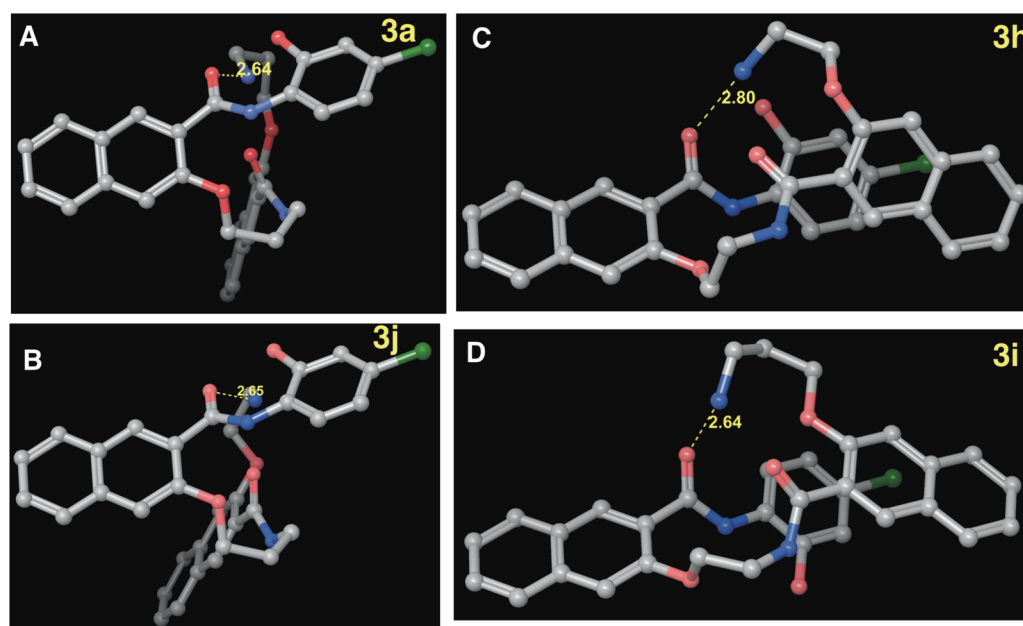


Figure 3. Conformation of the global energy minimum of **3a** (A), **3j** (B), **3h** (C), and **3i** (D). The distance between the amide oxygen and ammonium nitrogen was labeled in each conformation to indicate formation of an intramolecular hydrogen bond.

minima using MacroModel. The conformational ensemble was generated by systematically rotating all the rotatable bonds in **3a** and **3h–j**. The identified global conformational minima are shown in Figure 3. All the four compounds form an intramolecular hydrogen bond between the protonated ammonium nitrogen and amide carbonyl oxygen. However, the more potent CREB inhibitors **3h** and **3i** adopt a more compact conformation by forming π – π stacking interaction between one of the naphthyl rings and chlorophenyl ring (Figure 3). On the other hand, the same naphthyl ring in the less potent compounds **3a** and **3j** do not form π – π stacking interaction with the chlorophenyl ring by assuming a more extended conformation at their global minima. These differences suggest that the unique conformation associated with **3h** and **3i** may contribute to their potent CREB inhibitory activity and antiproliferative activity.

Compound 3i Selectively Inhibited CREB-Mediated Gene Transcription. In the CREB RLuc reporter assay with transfected HEK 293T cells, compound **3i** was very potent in inhibiting CREB's transcription activity. In order to investigate if **3i** also inhibited endogenous CREB target gene expression, the transcript level of nuclear receptor related 1 protein (*Nurr1*/*NR4A2*), a well-defined CREB target gene in HEK 293T cells, was evaluated.^{17,32} The cells were treated with **3i** followed by stimulation with forskolin (10 μ M). Then the relative mRNA of *Nurr1*/*NR4A2* was determined by quantitative reverse transcription polymerase chain reaction (qRT-PCR). As shown in Figure 4, forskolin robustly stimulated *Nurr1*/*NR4A2* level to ~31-fold. **3i** dose-dependently inhibited transcription of *Nurr1*/*NR4A2*. Significant inhibition was observed even at 50 nM of **3i**. In contrast, the weaker CREB inhibitor **3a** only started to show significant inhibition at 1000 nM (Figure S1 in Supporting Information). These results are consistent with those from the CREB reporter assay.

To investigate **3i**'s selectivity on different transcription activators, we employed RLuc reporter assays to monitor individual transcription factor activity in HEK 293T cells.

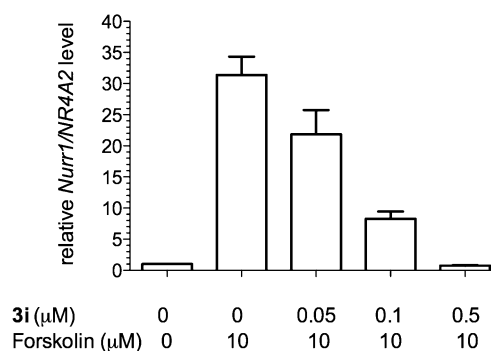


Figure 4. Compound **3i** decreased endogenous CREB target gene expression. HEK 293T cells were treated with different concentrations of **3i** followed by treatment with forskolin. Then the relative mRNA level of *Nurr1*/*NR4A2* was determined by qRT-PCR analysis.

VP16-CREB is a fusion protein by fusing the potent activation domain VP16 to the full-length CREB. It requires CREB-CRE interaction for transcriptional activation, but it is a constitutively active transcription factor independent of phosphorylation as opposed to wild type CREB.³³ As shown in Table 1 and Figure S5, **3i** potently (IC_{50} = 81 nM) and efficaciously inhibited CREB's transcription activity in HEK 293T cells. On the other hand, it showed much less efficacious inhibition of VP16-CREB and p53-mediated gene transcription. And even this weak inhibition only occurred at high concentrations (>1 μ M). In a separate transcription reporter assay with NF- κ B, much higher concentrations of **3i** were required to inhibit NF- κ B-mediated gene transcription (IC_{50} = 5290 nM, Figure S2), which is distinct from **1** and its phosphate.³² Collectively, these results indicate that **3i** selectively inhibited CREB-mediated gene transcription.

Compound 3i Selectively Inhibited the Growth of Cancer Cells but Not Normal Cells. With a potent and specific CREB inhibitor **3i** in hand, we tested if it was toxic to normal cells. Previous genetic studies have shown that normal cells tolerate well with reduced levels of CREB.^{34,35} As shown

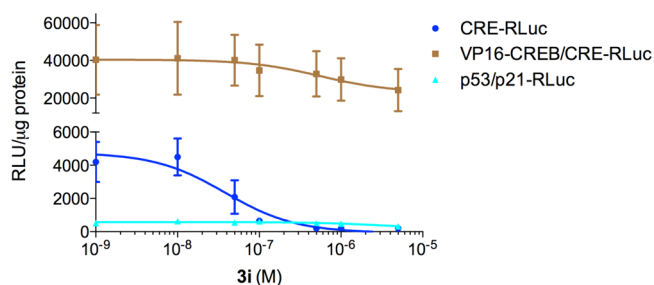


Figure 5. Compound **3i** selectively inhibited CREB-mediated gene transcription. HEK 293T cells were transfected with indicated combinations of plasmids. Then the cells were treated with different concentrations of **3i** before RLuc activity measurement. Forskolin (Fsk, 10 μ M) was added to CRE-RLuc only transfected cells at 30 min after drug treatment to stimulate CREB's activity. The RLuc activity was normalized to the protein concentration and presented as relative luciferase unit (RLU)/ μ g protein.

in Table 2 and Figure 6A,B, **3i** potently inhibited growth of MDA-MB-231 and MDA-MB-468 cells with GI_{50} in the midnanomolar concentration range. On the other hand, no significant inhibition of growth was observed in two different normal cell lines, human mammary epithelial cells (HMEC) and human foreskin fibroblasts (HFF), up to 1 μ M concentration, which is more than 10-fold higher than its GI_{50} in MDA-MB-231 and MDA-MB-468 breast cancer cells. This selective toxicity is in strong contrast to conventional chemotherapeutics like doxorubicin, which did not show differential toxicity between cancer and normal cells under the same assay conditions.³⁶ Therefore, pharmacological inhibition of CREB's transcription activity is well tolerated in normal cells, which is consistent with the idea of cancer cells' addiction to CREB.^{3,37,38}

Compound **3i Completely Suppressed the Tumor Growth in Vivo.** The selective in vitro toxicity of **3i** against

cancer cells versus normal cells prompted us to investigate its in vivo antitumor activity. Preliminary toxicity studies showed that intraperitoneal (ip) injection of 10 mg/kg of **3i** is well tolerated in mice (Figure S3). This dose was chosen for in vivo antitumor efficacy studies in the MDA-MB-468 xenografts. The MDA-MB-468 tumor was allowed to grow to an average size of 100 mm³ in nude mice. Then the mice were randomized to receive either vehicle or **3i** at 10 mg/kg once a day, 5 days per week for 5 weeks by ip injection. The tumor volumes and body weights were measured 2–3 times/week. The data in Figure 7A showed the tumor growth in the mice treated with **3i** was efficaciously inhibited with complete tumor stasis. During the same period, the tumor volume in the vehicle-treated group was more than tripled (Figure 7A). The body weights of **3i**-treated animals and vehicle-treated ones were indistinguishable from each other during the entire treatment period (Figure 7B), indicating no overt toxicity with this compound treatment. These results are consistent with in vitro studies with compound **3i** (Figure 6C,D) where normal cells could tolerate much higher concentrations of **3i** than cancer cells. These data further support the notion that pharmacologically targeting CREB is a promising strategy for development of novel cancer therapeutics.

CONCLUSION

In an important extension of previous work,¹⁷ we have prepared a series of naphthamide derivatives based on the structure of **3a**. Overall, the observed antiproliferative activities of these naphthamides correlated well with their CREB inhibition activity. Structure–activity relationships observed for members of this series revealed that many structural elements present in **3a** are crucial for maintaining CREB inhibition and cancer cell growth inhibition activity. The phenol in the chlorophenyl ring, the primary amino group in the side chain, and two naphthyl rings in **3a** are all important for maintaining **3a**'s bioactivity. Importantly, the carbon chain

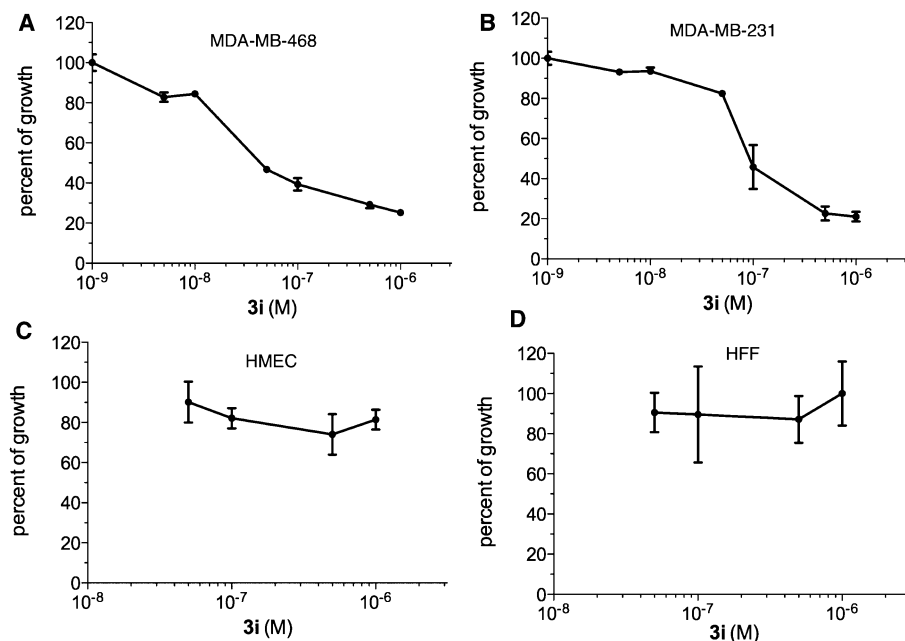


Figure 6. Compound **3i** selectively inhibited tumor cell growth. Shown are antiproliferative dose–response curves of **3i** in breast cancer MDA-MB-468 (A) and MDA-MB-231 (B) cells as well as normal HMEC (C) and HFF (D) cells. The cells were incubated with **3i** for 72 h, and then the remaining live cells were quantified by the MTT assay.

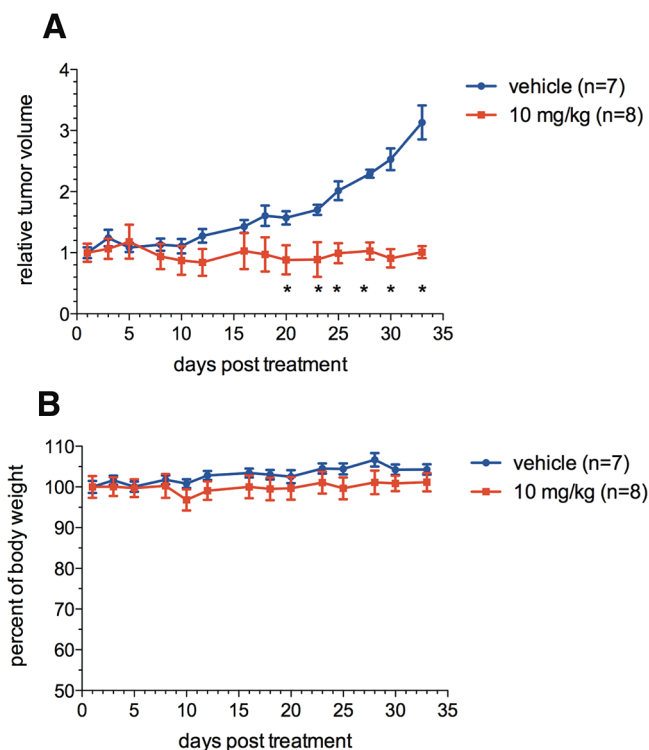


Figure 7. Compound **3i** suppressed MDA-MB-468 tumor growth in vivo. MDA-MB-468 tumor-bearing mice were treated either with vehicle or with **3i** at 10 mg/kg once a day for 5 days a week. The duration of treatment was 5 weeks. The relative tumor volume (A) and body weight (B) of the treated mice are shown: (*) $P < 0.05$ by Student's t test.

length of the linker between the two naphthyl rings, and the carbon chain length of the side chain are absolutely critical for optimal activities. We identified compound **3i**, which we named as **666-15**, as a potent and efficacious inhibitor toward CREB-mediated gene transcription. **666-15** also displayed potent and efficacious growth inhibition activity against cancer cells in vitro and in vivo. **666-15** should give us a new tool to further investigate CREB signaling.³⁹

EXPERIMENT SECTION

Chemistry. General. Glass Contout solvent purification system was used to purify all the anhydrous solvents to be used for reactions. Melting points were determined in capillary tubes using Mel-Temp and are uncorrected. All ^1H and ^{13}C NMR spectra were obtained in a Bruker Avance 400 MHz spectrometer using CDCl_3 or $\text{DMSO}-d_6$ as the solvent, and the chemical shifts of the residual CHCl_3 (δ 7.24) or DMSO (δ 2.50) were taken as references. Chemical shifts (δ) are reported in parts per million (ppm), and the signals are described as brs (broad singlet), d (doublet), dd (doublet of doublet), td (triplet of doublet), m (multiplet), q (quartet), s (singlet), and t (triplet). Coupling constants (J values) are given in Hz. Silica gel flash chromatography was performed using 230–400 mesh silica gel (EMD). All reactions were monitored using thin-layer chromatography (TLC) on silica gel plates (EMD). Yields were of purified compounds. All final compounds for biological evaluations were confirmed to be of >95% purity based on reverse phase HPLC (Waters, Milford, MA) analysis using an XBridge C18 column (4.6 mm \times 150 mm) and detected at 254 nm. The mobile phases for HPLC are water and acetonitrile, both of which contained 0.1% TFA. The mass spectra were obtained from a Thermo Electron LTQ-Orbitrap Discovery high resolution mass spectrometer (Thermo

Scientific) with electrospray operated in either positive or negative mode.

General Procedure A: Mitsunobu Reaction. To a solution of phenol (1 equiv), alcohol (1.2–1.5 equiv), and PPh_3 (1.2–1.5 equiv) in THF (1.5–2 mL/mmol) was added DEAD (1.2–1.5 equiv) in THF (0.2–0.3 mL/mmol) dropwise at 0 $^\circ\text{C}$. The reaction mixture was stirred at room temperature overnight. The solvent was removed under reduced pressure and the residue was purified by silica gel flash column chromatography to give the corresponding product.

General Procedure B: Saponification of the Methyl Esters with LiOH. To a solution of methyl ester (1 equiv) in MeOH–THF–water (1:1:1, 9 mL/mmol) was added LiOH·H₂O (5 equiv) at room temperature. The resulting mixture was stirred at room temperature overnight. The organic solvents were removed under reduced pressure, and the residue was acidified with 2 N HCl at 0 $^\circ\text{C}$ to pH \sim 2 (pH \sim 7 for **5e**). The reaction mixture was extracted with ethyl acetate or THF for **5e**. The organic layer was separated and washed with brine and dried over Na_2SO_4 . The solution was filtered and the solvent was evaporated to give the corresponding acid.

General Procedure C: Amide Formation by MsCl and TEA. To a stirred solution of **5** (1 equiv) and TEA (1.0 equiv) in THF (3 mL/mmol) was added MsCl (1 equiv) dropwise at 0 $^\circ\text{C}$. The reaction mixture was stirred at 0 $^\circ\text{C}$ for 30 min, when the corresponding ammonium salt **7** or aniline **9** (1 equiv) was added. The reaction mixture was stirred at room temperature overnight. Another portion of TEA (1.0 equiv) was added if the salt **7** was used. The reaction mixture was diluted with 5% NaHCO_3 and extracted with ethyl acetate. The organic layer was separated, washed with brine, and dried over Na_2SO_4 . The solution was filtered and the solvent was removed to give a residue, which was purified by silica gel flash column chromatography to yield the corresponding amide.

General Procedure D: Removal of the Boc and MOM with 2 N HCl. An HCl solution in Et₂O (2 M, 2–10 equiv) was added to a stirred solution of **6** or **8** (1.0 equiv) in CHCl_3 –MeOH (1:1, 6–10 mL/mmol). The resulting mixture was stirred at room temperature overnight. The solvents were removed under reduced pressure, and the solid was treated with acetone or ethyl ether. The solid was collected by filtration to give the corresponding product.

3-(3-Aminopropoxy)-N-(3-((4-chlorophenyl)carbamoyl)naphthalen-2-yl)oxy)propyl)-2-naphthamide Hydrochloride (3b**).** Compound **3b** (33 mg, 83%) was obtained as a white solid from **8b** following general procedure D: mp 247–248 $^\circ\text{C}$. ^1H NMR (400 MHz, $\text{DMSO}-d_6$) δ 10.49 (s, 1 H), 8.59 (t, J = 5.7 Hz, 1 H), 8.20 (s, 1 H), 8.05 (s, 1 H), 8.00 (brs, 3 H), 7.96 (d, J = 8.1 Hz, 1 H), 7.89 (d, J = 7.9 Hz, 1 H), 7.87 (d, J = 8.4 Hz, 1 H), 7.85 (d, J = 8.3 Hz, 1 H), 7.81 (d, J = 8.9 Hz, 2 H), 7.58–7.50 (m, 3 H), 7.45–7.36 (m, 5 H), 4.31 (t, J = 5.9 Hz, 2 H), 4.26 (t, J = 5.8 Hz, 2 H), 3.52 (q, J = 6.1 Hz, 2 H), 3.00 (q, J = 5.5 Hz, 2 H), 2.10 (quintet, J = 5.8 Hz, 4 H); ^{13}C NMR (100 MHz, $\text{DMSO}-d_6$) δ 167.01, 165.23, 153.75, 153.57, 138.58, 135.46, 135.12, 130.46, 129.93, 129.17, 128.78, 128.62, 128.24, 128.05, 127.95, 127.56, 127.45, 127.15, 126.99, 126.90, 124.83, 124.81, 121.54, 107.81, 107.71, 66.36, 66.32, 37.20, 36.52, 29.14, 26.79. HRESI-MS for $\text{C}_{34}\text{H}_{32}\text{ClN}_3\text{O}_4 + \text{H}$, calcd 582.21541, found 582.21557.

3-(3-Aminopropoxy)-N-(3-(2-((4-chloro-2-hydroxyphenyl)carbamoyl)phenoxy)propyl)-2-naphthamide Hydrochloride (3c**).** Compound **3c** (90 mg, 71%) was obtained as a white solid from **8c** following general procedure D: mp 179–180 $^\circ\text{C}$. ^1H NMR (400 MHz, $\text{DMSO}-d_6$) δ 11.05 (s, 1 H), 10.44 (s, 1 H), 8.61 (t, J = 5.8 Hz, 1 H), 8.43 (d, J = 9.0 Hz, 1 H), 8.11 (dd, J = 7.8, 1.9 Hz, 1 H), 8.06 (s, 1 H), 8.01 (brs, 3 H), 7.89 (d, J = 8.1 Hz, 1 H), 7.84 (d, J = 8.2 Hz, 1 H), 7.59 (td, J = 7.9, 1.7 Hz, 1 H), 7.52 (t, J = 7.1 Hz, 1 H), 7.43 (s, 1 H), 7.40 (t, J = 7.8 Hz, 1 H), 7.30 (d, J = 8.5 Hz, 1 H), 7.14 (t, J = 7.6 Hz, 1 H), 7.05 (d, J = 2.2 Hz, 1 H), 6.87 (dd, J = 8.8, 2.3 Hz, 1 H), 4.37 (t, J = 6.1 Hz, 2 H), 4.25 (t, J = 5.9 Hz, 2 H), 3.55 (q, J = 6.1 Hz, 2 H), 3.01 (q, J = 5.8 Hz, 2 H), 2.24 (quintet, J = 6.3 Hz, 2 H), 2.08 (quintet, J = 6.3 Hz, 2 H); ^{13}C NMR (100 MHz, $\text{DMSO}-d_6$) δ 166.59, 162.27, 156.72, 153.09, 147.55, 134.61, 133.69, 131.55, 129.42, 128.14, 127.55, 127.44, 126.71, 126.68, 126.42, 126.27, 124.30, 121.05, 120.92, 120.63, 118.66, 114.29, 113.29, 107.11, 67.23, 65.92, 36.85,

36.21, 28.66, 26.26. HRESI-MS for $C_{30}H_{30}ClN_3O_5 + H$, calcd 548.19468, found 548.19474.

3-(3-(2-(3-Aminopropoxy)benzamido)propoxy)-N-(4-chloro-2-hydroxyphenyl)-2-naphthamide Hydrochloride (3d). Compound 3d (12 mg, 53%) was obtained as a white solid from 8d following general procedure D: mp 157–158 °C. 1H NMR (400 MHz, DMSO- d_6) δ 10.94 (s, 1 H), 10.50 (s, 1 H), 8.72 (s, 1 H), 8.46 (d, J = 8.7 Hz, 1 H), 8.38 (t, J = 6.0 Hz, 1 H), 8.04 (d, J = 8.3 Hz, 1 H), 7.90 (d, J = 7.8 Hz, 1 H), 7.88 (brs, 3 H), 7.62 (s, 1 H), 7.59 (td, J = 7.4, 1.0 Hz, 1 H), 7.54 (dd, J = 7.6, 1.8 Hz, 1 H), 7.45 (td, J = 7.8, 1.0 Hz, 1 H), 7.43 (t, J = 8.0, 1.2 Hz, 1 H), 7.09 (d, J = 8.3 Hz, 1 H), 7.02 (d, J = 2.6 Hz, 1 H), 7.00 (t, J = 7.4 Hz, 1 H), 6.92 (dd, J = 8.8, 2.5 Hz, 1 H), 4.42 (t, J = 6.1 Hz, 2 H), 4.14 (t, J = 5.8 Hz, 2 H), 3.54 (q, J = 6.1 Hz, 2 H), 2.95 (q, J = 6.1 Hz, 2 H), 2.26 (quintet, J = 6.2 Hz, 2 H), 2.01 (quintet, J = 6.0 Hz, 2 H); ^{13}C NMR (100 MHz, DMSO- d_6) δ 167.04, 162.70, 156.01, 154.08, 148.16, 136.12, 133.56, 132.13, 130.03, 129.41, 129.03, 128.06, 127.51, 126.85, 126.69, 125.22, 125.18, 123.00, 121.53, 120.99, 119.34, 114.84, 113.20, 108.55, 67.62, 66.41, 37.33, 36.62, 29.04, 26.81. HRESI-MS for $C_{30}H_{30}ClN_3O_5 + H$, calcd 548.19468, found 548.19467.

N-(4-Chloro-2-hydroxyphenyl)-3-(3-(3-(3-morpholinopropoxy)-2-naphthamido)propoxy)-2-naphthamide Hydrochloride (3e). Compound 3e (50 mg, 85%) was obtained as a white solid from 8e following general procedure D: mp 144–145 °C. 1H NMR (400 MHz, DMSO- d_6) δ 11.02 (s, 1 H), 10.55 (s, 1 H), 10.36 (brs, 1 H), 8.73 (s, 1 H), 8.53 (t, J = 5.6 Hz, 1 H), 8.44 (d, J = 8.8 Hz, 1 H), 8.09 (s, 1 H), 8.05 (d, J = 8.1 Hz, 1 H), 7.91 (d, J = 8.4 Hz, 1 H), 7.88 (d, J = 8.5 Hz, 1 H), 7.83 (d, J = 8.2 Hz, 1 H), 7.66 (s, 1 H), 7.59 (t, J = 7.5 Hz, 1 H), 7.53 (t, J = 7.5 Hz, 1 H), 7.45 (t, J = 7.5 Hz, 1 H), 7.44 (s, 1 H), 7.39 (t, J = 7.6 Hz, 1 H), 7.02 (d, J = 2.1 Hz, 1 H), 6.88 (dd, J = 8.8, 2.4 Hz, 1 H), 4.47 (t, J = 6.0 Hz, 2 H), 4.23 (t, J = 5.8 Hz, 2 H), 3.82–3.71 (m, 4 H), 3.62 (q, J = 5.7 Hz, 2 H), 3.40–3.33 (m, 2 H), 3.23 (q, J = 6.3 Hz, 2 H), 2.95 (q, J = 10.2 Hz, 2 H), 2.31 (quintet, J = 6.3 Hz, 2 H), 2.19 (quintet, J = 6.4 Hz, 2 H); ^{13}C NMR (100 MHz, DMSO- d_6) δ 166.14, 162.12, 153.63, 153.03, 147.68, 135.66, 134.62, 133.13, 129.72, 128.94, 128.55, 127.55, 127.53, 126.55, 126.41, 126.38, 126.19, 124.69, 124.34, 122.41, 120.92, 118.76, 114.32, 108.10, 107.45, 67.30, 65.81, 62.94, 53.84, 51.06, 36.36, 28.64, 22.47. HRESI-MS for $C_{38}H_{38}ClN_3O_6 + H$, calcd 668.25219, found 668.25229.

N-(4-Chloro-2-hydroxyphenyl)-3-(3-(3-(3-(methylamino)propoxy)-2-naphthamido)propoxy)-2-naphthamide Hydrochloride (3f). Compound 3f (75 mg, 92%) was obtained as a white solid from 8f following general procedure D: mp 139–140 °C. 1H NMR (400 MHz, DMSO- d_6) δ 11.06 (s, 1 H), 10.55 (s, 1 H), 8.73 (s, 1 H), 8.71 (t, J = 5.7 Hz, 1 H), 8.66 (brs, 2 H), 8.46 (d, J = 8.4 Hz, 1 H), 8.08 (s, 1 H), 8.05 (d, J = 7.7 Hz, 1 H), 7.91 (d, J = 8.3 Hz, 1 H), 7.88 (d, J = 7.6 Hz, 1 H), 7.83 (d, J = 8.1 Hz, 1 H), 7.66 (s, 1 H), 7.59 (t, J = 7.5 Hz, 1 H), 7.53 (t, J = 7.5 Hz, 1 H), 7.44 (t, J = 8.4 Hz, 1 H), 7.43 (s, 1 H), 7.40 (t, J = 7.2 Hz, 1 H), 7.05 (d, J = 2.2 Hz, 1 H), 6.90 (dd, J = 8.6, 2.1 Hz, 1 H), 4.47 (t, J = 5.5 Hz, 2 H), 4.24 (t, J = 5.2 Hz, 2 H), 3.60 (q, J = 5.6 Hz, 2 H), 3.06 (t, J = 6.2 Hz, 2 H), 2.49 (s, 3 H), 2.31 (quintet, J = 5.9 Hz, 2 H), 2.10 (quintet, J = 6.0 Hz, 2 H); ^{13}C NMR (100 MHz, DMSO- d_6) δ 166.88, 162.13, 153.62, 153.02, 147.71, 135.67, 134.63, 133.12, 129.47, 128.93, 128.54, 128.15, 127.62, 127.55, 127.43, 126.95, 126.44, 126.39, 126.20, 124.68, 124.37, 122.40, 120.89, 118.74, 114.35, 108.13, 107.15, 67.22, 66.25, 46.53, 36.29, 32.50, 28.55, 24.79. HRESI-MS for $C_{33}H_{34}ClN_3O_5 + H$, calcd 612.22598, found 612.22608.

N-(4-Chloro-2-hydroxyphenyl)-3-(3-(3-(3-hydroxypropoxy)-2-naphthamido)propoxy)-2-naphthamide (3g). Compound 3g (80 mg, 95%) was obtained as a white solid from 8g following general procedure D: mp 139–140 °C. 1H NMR (400 MHz, DMSO- d_6) δ 10.88 (s, 1 H), 10.53 (s, 1 H), 8.73 (s, 1 H), 8.53 (t, J = 5.8 Hz, 1 H), 8.45 (d, J = 8.8 Hz, 1 H), 8.20 (s, 1 H), 8.05 (d, J = 8.9 Hz, 1 H), 7.92–7.87 (m, 2 H), 7.83 (d, J = 8.2 Hz, 1 H), 7.63 (s, 1 H), 7.59 (t, J = 7.6 Hz, 1 H), 7.51 (t, J = 7.5 Hz, 1 H), 7.44 (t, J = 7.0 Hz, 1 H), 7.43 (s, 1 H), 7.37 (t, J = 7.6 Hz, 1 H), 6.98 (d, J = 2.3 Hz, 1 H), 6.89 (dd, J = 8.7, 2.3 Hz, 1 H), 4.45 (t, J = 6.2 Hz, 2 H), 4.21 (t, J = 6.0 Hz, 2 H), 3.59 (q, J = 6.0 Hz, 2 H), 3.52 (t, J = 5.8 Hz, 2 H), 2.30 (quintet, J = 5.9 Hz, 2 H), 1.90 (quintet, J = 5.7 Hz, 2 H); ^{13}C NMR (100 MHz,

DMSO- d_6) δ 165.85, 162.64, 154.16, 148.18, 136.15, 135.39, 133.61, 130.92, 129.40, 128.99, 128.78, 128.06, 127.90, 127.48, 126.84, 126.71, 126.14, 125.14, 124.62, 122.93, 121.50, 119.27, 114.81, 108.51, 107.52, 67.74, 66.65, 58.40, 36.65, 32.10, 29.16. HRESI-MS for $C_{34}H_{31}ClN_2O_6 + Na$, calcd 621.17628, found 621.17501.

3-(2-Aminoethoxy)-N-(2-((3-(4-chloro-2-hydroxyphenyl)-carbamoyl)naphthalen-2-yl)oxy)ethyl)-2-naphthamide Hydrochloride (3h). Compound 3h (48 mg, 89%) was obtained as a white solid from 8h following general procedure D: mp 265–266 °C. 1H NMR (400 MHz, DMSO- d_6) δ 11.02 (s, 1 H), 10.58 (s, 1 H), 8.77–8.73 (m, 2 H), 8.45 (d, J = 8.8 Hz, 1 H), 8.25 (brs, 3 H), 8.13 (s, 1 H), 8.06 (d, J = 8.1 Hz, 1 H), 7.93 (d, J = 8.4 Hz, 1 H), 7.86 (d, J = 8.0 Hz, 1 H), 7.79 (d, J = 8.0 Hz, 1 H), 7.75 (s, 1 H), 7.61 (td, J = 7.7, 1.0 Hz, 1 H), 7.55 (s, 1 H), 7.55 (td, J = 7.5, 1.0 Hz, 1 H), 7.46 (td, J = 7.4, 1.0 Hz, 1 H), 7.41 (td, J = 7.6, 1.1 Hz, 1 H), 7.01 (d, J = 2.2 Hz, 1 H), 6.90 (dd, J = 8.1, 2.4 Hz, 1 H), 4.54 (t, J = 6.3 Hz, 2 H), 4.41 (t, J = 4.9 Hz, 2 H), 3.98 (q, J = 6.2 Hz, 2 H), 3.29–3.32 (m, 2 H); ^{13}C NMR (100 MHz, DMSO- d_6) δ 166.21, 162.09, 153.11, 152.64, 147.78, 135.66, 134.74, 133.15, 130.66, 128.92, 128.53, 128.24, 127.86, 127.74, 127.70, 127.05, 126.50, 126.20, 125.98, 124.79, 124.69, 122.47, 120.99, 118.79, 114.38, 108.67, 108.38, 67.19, 65.66, 38.41, 38.21. HRESI-MS for $C_{32}H_{28}ClN_3O_5 + H$, calcd 570.17903, found 570.17881.

3-(3-Aminopropoxy)-N-(2-((3-(4-chloro-2-hydroxyphenyl)-carbamoyl)naphthalen-2-yl)oxy)ethyl)-2-naphthamide Hydrochloride (3i or 666-15). Compound 3i (35 mg, 65%) was obtained as a white solid from 8i following general procedure D: mp 209–210 °C. 1H NMR (400 MHz, DMSO- d_6) δ 11.05 (s, 1 H), 10.59 (s, 1 H), 8.78 (t, J = 5.7 Hz, 1 H), 8.75 (s, 1 H), 8.47 (d, J = 9.1 Hz, 1 H), 8.07 (d, J = 8.7 Hz, 1 H), 8.05 (s, 1 H), 7.93 (d, J = 8.3 Hz, 1 H), 7.90 (brs, 3 H), 7.83 (d, J = 8.3 Hz, 1 H), 7.74 (s, 1 H), 7.72 (d, J = 7.7 Hz, 1 H), 7.61 (td, J = 7.6, 1.1 Hz, 1 H), 7.53 (td, J = 7.6, 1.2 Hz, 1 H), 7.46 (td, J = 7.5, 1.0 Hz, 1 H), 7.43 (s, 1 H), 7.38 (td, J = 7.6, 1.2 Hz, 1 H), 7.02 (d, J = 2.2 Hz, 1 H), 6.92 (dd, J = 8.7, 2.4 Hz, 1 H), 4.53 (t, J = 6.2 Hz, 2 H), 4.24 (t, J = 5.7 Hz, 2 H), 3.96 (q, J = 5.9 Hz, 2 H), 3.01–2.93 (m, 2 H), 2.06 (quintet, J = 6.3 Hz, 2 H); ^{13}C NMR (100 MHz, DMSO- d_6) δ 166.56, 162.10, 153.12, 153.05, 147.76, 135.65, 134.77, 133.19, 130.00, 128.93, 128.56, 128.15, 127.78, 127.70, 127.36, 127.04, 126.50, 126.41, 125.69, 124.81, 124.39, 122.44, 120.98, 118.83, 114.41, 108.36, 107.32, 67.46, 65.99, 38.41, 36.84, 26.14. HRESI-MS for $C_{33}H_{30}ClN_3O_5 + H$, calcd 584.19468, found 584.19456.

3-(2-Aminoethoxy)-N-(3-((3-(4-chloro-2-hydroxyphenyl)-carbamoyl)naphthalen-2-yl)oxy)propyl)-2-naphthamide Hydrochloride (3j). Compound 3j (44 mg, 90%) was obtained as a white solid from 8j following general procedure D: mp 200–201 °C. 1H NMR (400 MHz, DMSO- d_6) δ 11.00 (s, 1 H), 10.56 (s, 1 H), 8.73 (s, 1 H), 8.64 (t, J = 5.9 Hz, 1 H), 8.47 (d, J = 9.0 Hz, 1 H), 8.17 (brs, 3 H), 8.14 (s, 1 H), 8.05 (d, J = 8.0 Hz, 1 H), 7.91 (d, J = 8.4 Hz, 2 H), 7.86 (d, J = 8.6 Hz, 1 H), 7.66 (s, 1 H), 7.59 (t, J = 7.7 Hz, 1 H), 7.56 (s, 1 H), 7.55 (t, J = 7.0 Hz, 1 H), 7.45 (t, J = 7.8 Hz, 1 H), 7.42 (td, J = 7.1 Hz, 1 H), 7.03 (d, J = 2.6 Hz, 1 H), 6.90 (dd, J = 8.8, 2.4 Hz, 1 H), 4.47 (t, J = 5.9 Hz, 2 H), 4.41 (t, J = 4.7 Hz, 2 H), 3.61 (q, J = 5.7 Hz, 2 H), 3.22–3.29 (m, 2 H), 2.32 (quintet, J = 6.1 Hz, 2 H); ^{13}C NMR (100 MHz, DMSO- d_6) δ 166.26, 162.15, 153.63, 152.66, 147.71, 135.68, 134.61, 133.14, 130.26, 128.93, 128.53, 128.23, 127.83, 127.72, 127.56, 126.97, 126.75, 126.51, 126.41, 126.22, 124.68, 122.39, 120.92, 118.77, 114.34, 108.83, 108.14, 67.34, 65.70, 38.29, 36.46, 28.55. HRESI-MS for $C_{33}H_{30}ClN_3O_5 + H$, calcd 584.19468, found 584.19433.

tert-Butyl (3-((3-(4-Chlorophenyl)carbamoyl)naphthalen-2-yl)oxy)propyl)carbamate (6b). Compound 6b (700 mg, 77%) was prepared as a white solid from 1 (596 mg, 2 mmol) and A1 (420 mg, 2.4 mmol) following general procedure A. The product was eluted from the column with hexanes–ethyl acetate (4:1 to 2:1): mp 134–135 °C. 1H NMR (400 MHz, $CDCl_3$) δ 9.98 (s, 1 H), 8.63 (s, 1 H), 7.83 (d, J = 8.0 Hz, 1 H), 7.67 (d, J = 8.4 Hz, 2 H), 7.63 (d, J = 8.8 Hz, 1 H), 7.45 (t, J = 8.4 Hz, 1 H), 7.35 (t, J = 7.6 Hz, 1 H), 7.27 (d, J = 8.4 Hz, 2 H), 7.10 (s, 1 H), 4.87 (brs, 1 H), 4.21 (t, J = 5.2 Hz, 2 H), 3.37 (q, J = 6.0 Hz, 2 H), 2.06 (quintet, J = 5.6 Hz, 2 H), 1.36 (s, 9 H). HRESI-MS for $C_{25}H_{27}ClN_2O_4 + Na$, calcd 477.15516, found 477.15411.

tert-Butyl (3-(2-((4-Chloro-2-hydroxyphenyl)carbamoyl)phenoxy)propyl)carbamate (6c). Compound 6c (0.89 g, 59%) was prepared as a white solid from 5c (1.06 g, 3.6 mmol) and 9 (0.515 g, 3.6 mmol) following general procedure C. The product was eluted from the column with dichloromethane–ethyl acetate (20:1): mp 147–148 °C. ¹H NMR (400 MHz, CDCl₃) δ 10.48 (s, 1 H), 9.81 (brs, 1 H), 8.26 (dd, *J* = 7.9, 1.9 Hz, 1 H), 7.91 (d, *J* = 7.1 Hz, 1 H), 7.48 (td, *J* = 7.7, 2.1 Hz, 1 H), 7.12 (td, *J* = 7.6, 1.2 Hz, 1 H), 7.00 (d, *J* = 8.5 Hz, 1 H), 6.96 (d, *J* = 2.2 Hz, 1 H), 6.89 (dd, *J* = 8.6, 2.2 Hz, 1 H), 4.86 (brs, 1 H), 4.22 (t, *J* = 5.4 Hz, 2 H), 3.40 (q, *J* = 6.1 Hz, 2 H), 2.16 (quintet, *J* = 5.1 Hz, 2 H), 1.45 (s, 9 H); ¹³C NMR (100 MHz, CDCl₃) δ 163.37, 156.45, 156.32, 147.33, 133.03, 132.00, 128.95, 126.13, 121.32, 121.03, 120.70, 119.93, 116.87, 111.56, 79.95, 66.68, 38.15, 29.68, 27.86. HRESI-MS for C₂₁H₂₅ClN₂O₅ + H, calcd 421.15248, found 421.15243.

tert-Butyl (2-((3-((4-Chloro-2-hydroxyphenyl)carbamoyl)naphthalen-2-yl)oxy)ethyl)carbamate (6h). Compound 6h (1.63 g, 60%) was prepared as a white solid from 5h (1.987 g, 6 mmol) and 9 (0.86 g, 6 mmol) following general procedure C. The product was eluted from the column with dichloromethane–ethyl acetate (10:1): mp 185–186 °C. ¹H NMR (400 MHz, DMSO-*d*₆) δ 10.87 (s, 1 H), 10.46 (s, 1 H), 8.72 (s, 1 H), 8.44 (d, *J* = 8.5 Hz, 1 H), 8.04 (d, *J* = 7.7 Hz, 1 H), 7.90 (d, *J* = 8.4 Hz, 1 H), 7.66 (s, 1 H), 7.60 (t, *J* = 7.5 Hz, 1 H), 7.45 (t, *J* = 7.5 Hz, 1 H), 7.07 (t, *J* = 5.7 Hz, 1 H), 6.96 (d, *J* = 2.3 Hz, 1 H), 6.91 (dd, *J* = 8.4, 2.2 Hz, 1 H), 4.31 (t, *J* = 6.5 Hz, 2 H), 3.59 (q, *J* = 6.2 Hz, 2 H), 1.35 (s, 9 H); ¹³C NMR (100 MHz, DMSO-*d*₆) δ 162.01, 155.66, 153.18, 147.74, 135.64, 133.15, 128.89, 128.49, 127.64, 126.99, 126.43, 126.23, 124.73, 122.34, 121.08, 118.79, 114.31, 108.19, 77.96, 67.94, 38.98, 28.13. HRESI-MS for C₂₄H₂₅ClN₂O₅ + Na, calcd 479.13442, found 479.13402.

3-(3-Aminopropoxy)-*N*-(4-chlorophenyl)-2-naphthamide (7b). The hydrochloride salt (500 mg, 83%) of 7b was obtained from 6b following general procedure D. The free amine 7b was obtained by neutralizing the hydrochloride salt with 5% NaHCO₃ solution and was extracted with CHCl₃. The CHCl₃ solution was dried over Na₂SO₄. The solvent was removed to give the free amine 7b in a quantitative yield: mp 234–235 °C. ¹H NMR (400 MHz, DMSO-*d*₆) δ 10.36 (s, 1 H), 8.20 (s, 1 H), 7.96 (d, *J* = 8.0 Hz, 1 H), 7.87 (d, *J* = 8.4 Hz, 1 H), 7.79 (d, *J* = 8.0 Hz, 2 H), 7.54 (t, *J* = 7.4 Hz, 1 H), 7.51 (s, 1 H), 7.42 (d, *J* = 8.8 Hz, 2 H), 7.39 (t, *J* = 6.8 Hz, 1 H), 4.26 (t, *J* = 6.0 Hz, 2 H), 2.72 (t, *J* = 6.4 Hz, 2 H), 1.88 (quintet, *J* = 6.0 Hz, 2 H); ¹³C NMR (100 MHz, DMSO-*d*₆) δ 165.59, 153.43, 138.53, 135.30, 130.02, 129.18, 128.73, 128.29, 127.96, 127.69, 127.58, 126.99, 124.96, 121.66, 107.75, 66.04, 37.17, 27.14. HRESI-MS for C₂₀H₁₉ClN₂O₂ + H, calcd 355.12078, found 355.12104.

2-(3-Aminopropoxy)-*N*-(4-chloro-2-hydroxyphenyl)-benzamide Hydrochloride (7c). Compound 7c (570 mg, 80%) was obtained as an off-white solid from 6c following general procedure D: mp 301–302 °C. ¹H NMR (400 MHz, DMSO-*d*₆) δ 11.05 (s, 1 H), 10.32 (s, 1 H), 8.41 (d, *J* = 8.7 Hz, 1 H), 8.09 (dd, *J* = 7.8, 1.7 Hz, 1 H), 8.01 (brs, 3 H), 7.59 (td, *J* = 5.8, 1.8 Hz, 1 H), 7.26 (d, *J* = 8.4 Hz, 1 H), 7.16 (t, *J* = 7.5 Hz, 1 H), 7.05 (d, *J* = 1.4 Hz, 1 H), 6.89 (dd, *J* = 8.6, 2.2 Hz, 1 H), 4.36 (t, *J* = 5.7 Hz, 2 H), 3.04 (q, *J* = 6.2 Hz, 2 H), 2.23 (quintet, *J* = 6.5 Hz, 2 H); ¹³C NMR (100 MHz, DMSO-*d*₆) δ 162.22, 156.37, 147.32, 133.62, 131.51, 126.75, 126.23, 121.22, 121.03, 120.58, 118.83, 114.27, 113.21, 66.26, 36.49, 26.59. HRESI-MS for C₁₆H₁₇ClN₂O₃ + H, calcd 321.10005, found 321.10001.

3-(2-Aminoethoxy)-*N*-(4-chloro-2-hydroxyphenyl)-2-naphthamide Hydrochloride (7h). Compound 7h (1.39 g, 97%) was obtained as a white solid from 6h following general procedure D: mp 305–306 °C. ¹H NMR (400 MHz, DMSO-*d*₆) δ 11.05 (s, 1 H), 10.29 (s, 1 H), 8.68 (s, 1 H), 8.41 (d, *J* = 8.6 Hz, 1 H), 8.28 (brs, 3 H), 8.06 (d, *J* = 8.0 Hz, 1 H), 7.94 (d, *J* = 8.2 Hz, 1 H), 7.66 (s, 1 H), 7.61 (td, *J* = 7.6, 1.3 Hz, 1 H), 7.47 (td, *J* = 7.6, 1.0 Hz, 1 H), 7.03 (d, *J* = 2.7 Hz, 1 H), 6.93 (dd, *J* = 8.5, 2.5 Hz, 1 H), 4.56 (t, *J* = 4.9 Hz, 1 H), 3.51–3.46 (m, 2 H); ¹³C NMR (100 MHz, DMSO-*d*₆) δ 162.16, 152.71, 147.80, 135.41, 132.98, 128.86, 128.55, 127.79, 127.01, 126.49, 126.37, 124.93, 123.07, 121.17, 118.88, 114.63, 108.18, 65.88, 38.23. HRESI-MS for C₁₉H₁₇ClN₂O₃ + H, calcd 357.10005, found 357.10020.

tert-Butyl (3-((3-((3-((4-Chlorophenyl)carbamoyl)naphthalen-2-yl)oxy)propyl)carbamoyl)naphthalen-2-yl)oxy)propyl)carbamate (8b). DIPEA (26 μL, 0.15 mmol) and BOP (67 mg, 0.15 mmol) were sequentially added to a solution of 5a (52 mg, 0.15 mmol) in dichloromethane (4 mL) at room temperature. The resulting mixture was stirred at room temperature for 5 min. Then an additional portion of DIPEA (35 μL, 0.19 mmol) and 7b (53 mg, 0.15 mmol) were added. The resulting mixture was stirred at room temperature overnight. The solid precipitated from the reaction mixture was collected by filtration and washed with dichloromethane (20 mL) to give product 8b (68 mg, 67%) as a white solid: mp 160–161 °C. ¹H NMR (400 MHz, DMSO-*d*₆) δ 10.45 (s, 1 H), 8.41 (t, *J* = 5.2 Hz, 1 H), 8.22 (s, 1 H), 8.13 (s, 1 H), 7.96 (d, *J* = 8.4 Hz, 1 H), 7.87 (d, *J* = 8.2 Hz, 1 H), 7.86 (d, *J* = 7.5 Hz, 1 H), 7.83–7.78 (m, 3 H), 7.56–7.47 (m, 3 H), 7.44–7.34 (m, 5 H), 6.95 (t, *J* = 5.8 Hz, 1 H), 4.30 (t, *J* = 5.7 Hz, 2 H), 4.14 (t, *J* = 5.7 Hz, 2 H), 3.56 (q, *J* = 6.2 Hz, 2 H), 3.12 (q, *J* = 5.5 Hz, 2 H), 2.11 (quintet, *J* = 5.6 Hz, 2 H), 1.89 (quintet, *J* = 6.2 Hz, 2 H), 1.33 (s, 9 H); ¹³C NMR (100 MHz, DMSO-*d*₆) δ 166.23, 165.06, 156.27, 153.91, 153.75, 138.53, 135.47, 135.28, 130.69, 130.60, 129.15, 128.82, 128.72, 128.28, 128.03, 127.97, 127.92, 127.55, 127.27, 126.92, 126.82, 126.61, 124.84, 124.66, 121.52, 107.68, 107.59, 78.07, 66.31, 66.22, 37.26, 36.45, 29.35, 29.24, 28.65. HRESI-MS for C₃₉H₄₀ClN₃O₆ + H, calcd 682.26784, found 682.26830.

tert-Butyl (3-((3-((3-((4-Chloro-2-hydroxyphenyl)carbamoyl)phenoxy)propyl)carbamoyl)naphthalen-2-yl)oxy)propyl)carbamate (8c). Compound 8c (170 mg, 66%) was prepared as a white foam solid from 5a (138 mg, 0.4 mmol) and 7c (143 mg, 0.4 mmol) following general procedure C. The product was eluted from the column with dichloromethane–ethyl acetate (10:1): mp 170–171 °C. ¹H NMR (400 MHz, CDCl₃) δ 10.66 (s, 1 H), 8.67 (brs, 1 H), 8.67 (s, 1 H), 8.28 (dd, *J* = 7.9, 2.0 Hz, 1 H), 8.18 (d, *J* = 8.8 Hz, 1 H), 7.91 (d, *J* = 8.1 Hz, 1 H), 7.70 (d, *J* = 8.5 Hz, 1 H), 7.52 (t, *J* = 7.3 Hz, 1 H), 7.46 (t, *J* = 7.7 Hz, 1 H), 7.41 (t, *J* = 7.3 Hz, 1 H), 7.17 (s, 1 H), 7.11 (t, *J* = 7.4 Hz, 1 H), 7.06 (d, *J* = 2.1 Hz, 1 H), 6.99 (d, *J* = 8.2 Hz, 1 H), 6.85 (dd, *J* = 8.8, 2.2 Hz, 1 H), 4.78 (t, *J* = 7.4 Hz, 1 H), 4.29 (t, *J* = 5.5 Hz, 2 H), 4.23 (t, *J* = 5.8 Hz, 2 H), 3.83 (q, *J* = 6.7 Hz, 2 H), 3.35 (q, *J* = 6.2 Hz, 2 H), 2.37 (quintet, *J* = 6.0 Hz, 2 H), 2.02 (quintet, *J* = 6.1 Hz, 2 H), 1.40 (s, 9 H); ¹³C NMR (100 MHz, CDCl₃) δ 165.90, 162.88, 156.40, 156.01, 153.02, 146.95, 135.18, 132.86, 131.87, 128.48, 128.06, 127.86, 127.49, 126.50, 125.83, 124.13, 121.68, 120.93, 120.84, 120.72, 119.57, 115.85, 111.52, 106.64, 79.07, 67.38, 65.05, 38.13, 36.74, 29.12, 29.05, 27.87. HRESI-MS for C₃₅H₃₈ClN₃O₇ + Na, calcd 670.22905, found 670.22723.

tert-Butyl (3-((3-((3-((4-Chloro-2-hydroxyphenyl)carbamoyl)naphthalen-2-yl)oxy)propyl)carbamoyl)phenoxy)propyl)carbamate (8d). Compound 8d (60 mg, 40%) was prepared as a white solid from 5c (59 mg, 0.2 mmol) and 7a (82 mg, 0.2 mmol) following general procedure C. The product was eluted from the column with hexanes–ethyl acetate (1:1): mp 179–180 °C. ¹H NMR (400 MHz, DMSO-*d*₆) δ 10.81 (s, 1 H), 10.50 (s, 1 H), 8.72 (s, 1 H), 8.45 (d, *J* = 8.5 Hz, 1 H), 8.27 (t, *J* = 5.1 Hz, 1 H), 8.04 (d, *J* = 8.1 Hz, 1 H), 7.87 (d, *J* = 7.9 Hz, 1 H), 7.65 (d, *J* = 7.6 Hz, 1 H), 7.58 (t, *J* = 7.1 Hz, 1 H), 7.57 (s, 1 H), 7.46–7.39 (m, 2 H), 7.07 (d, *J* = 8.4 Hz, 1 H), 6.98 (t, *J* = 7.6 Hz, 1 H), 6.95 (d, *J* = 2.3 Hz, 1 H), 6.92–6.86 (m, 2 H), 4.42 (t, *J* = 6.3 Hz, 2 H), 4.03 (t, *J* = 6.1 Hz, 2 H), 3.58 (q, *J* = 6.6 Hz, 2 H), 3.04 (q, *J* = 6.4 Hz, 2 H), 2.28 (quintet, *J* = 5.5 Hz, 2 H), 1.80 (quintet, *J* = 6.2 Hz, 2 H), 1.29 (s, 9 H); ¹³C NMR (100 MHz, DMSO-*d*₆) δ 165.97, 162.60, 156.46, 156.24, 154.11, 148.25, 136.12, 133.62, 132.33, 130.70, 129.40, 128.96, 128.05, 127.49, 126.82, 126.73, 125.13, 124.22, 122.92, 121.51, 120.82, 119.23, 114.78, 113.06, 108.43, 78.04, 67.69, 66.09, 37.03, 36.58, 29.39, 29.12, 28.60. HRESI-MS for C₃₅H₃₈ClN₃O₇ + Na, calcd 670.22905, found 670.22757.

***N*-(4-Chloro-2-hydroxyphenyl)-3-(3-(3-morpholinopropoxy)-2-naphthamido)propoxy-2-naphthamide (8e).** Compound 8e (90 mg, 34%) was prepared as a white solid from 5e (126 mg, 0.40 mmol) and 7a (163 mg, 0.40 mmol) following general procedure C. When the reaction mixture was diluted with 5% NaHCO₃, the crude product was precipitated and collected, which was then purified by flash column chromatography, eluting with dichloro-

methane–methanol (20:1) to give the desired product: mp 247–248 °C. ¹H NMR (400 MHz, DMSO-*d*₆) δ 10.93 (s, 1 H), 10.52 (s, 1 H), 8.74 (s, 1 H), 8.44 (d, *J* = 9.4 Hz, 1 H), 8.37 (t, *J* = 5.9 Hz, 1 H), 8.14 (s, 1 H), 8.05 (d, *J* = 8.2 Hz, 1 H), 7.88 (d, *J* = 8.4 Hz, 2 H), 7.83 (d, *J* = 8.4 Hz, 1 H), 7.62 (s, 1 H), 7.59 (t, *J* = 7.6 Hz, 1 H), 7.51 (t, *J* = 7.7 Hz, 1 H), 7.45 (t, *J* = 7.5 Hz, 1 H), 7.40 (s, 1 H), 7.37 (t, *J* = 7.5 Hz, 1 H), 6.94 (d, *J* = 1.6 Hz, 1 H), 6.86 (dd, *J* = 8.5, 2.1 Hz, 1 H), 4.46 (t, *J* = 6.4 Hz, 2 H), 4.11 (t, *J* = 6.2 Hz, 2 H), 3.60 (q, *J* = 5.7 Hz, 2 H), 3.41–3.36 (m, 4 H), 2.31 (quintet, *J* = 5.9 Hz, 2 H), 2.25 (t, *J* = 7.1 Hz, 2 H), 2.16–2.08 (m, 4 H), 1.83 (quintet, *J* = 6.3 Hz, 2 H); ¹³C NMR (100 MHz, DMSO-*d*₆) δ 165.51, 162.06, 153.60, 153.47, 147.58, 135.65, 134.80, 133.22, 130.09, 128.96, 128.57, 128.23, 127.60, 127.53, 127.44, 126.95, 126.38, 126.35, 126.19, 126.03, 124.70, 124.17, 122.33, 120.92, 118.79, 114.19, 107.97, 107.10, 67.30, 66.62, 65.97, 54.68, 53.17, 36.13, 28.65, 25.49.

tert-Butyl (3-((3-((3-((4-Chloro-2-hydroxyphenyl)-carbamoyl)naphthalen-2-yl)oxy)propyl)carbamoyl)-naphthalen-2-yl)oxy)propyl(methyl)carbamate (8f). Compound 8f (110 mg, 34%) was prepared as a white solid from 5f (160 mg, 0.45 mmol) and 7a (183 mg, 0.45 mmol) following general procedure C. The product was eluted from the column with dichloromethane–methanol (20:1): mp 219–220 °C. ¹H NMR (400 MHz, CDCl₃) δ 10.86 (s, 1 H), 10.52 (s, 1 H), 8.88 (t, *J* = 5.6 Hz, 1 H), 8.85 (s, 1 H), 8.65 (s, 1 H), 8.27 (d, *J* = 8.9 Hz, 1 H), 7.92 (d, *J* = 8.5 Hz, 1 H), 7.89 (d, *J* = 8.2 Hz, 1 H), 7.72 (d, *J* = 8.1 Hz, 1 H), 7.70 (d, *J* = 8.0 Hz, 1 H), 7.55–7.48 (m, 2 H), 7.74–7.37 (m, 2 H), 7.24 (s, 1 H), 7.17 (s, 1 H), 7.08 (d, *J* = 2.2 Hz, 1 H), 6.90 (dd, *J* = 8.7, 2.2 Hz, 1 H), 4.40 (t, *J* = 5.2 Hz, 2 H), 4.18 (t, *J* = 5.2 Hz, 2 H), 3.89 (q, *J* = 5.6 Hz, 2 H), 3.48 (t, *J* = 5.9 Hz, 2 H), 2.88 (s, 3 H), 2.44 (quintet, *J* = 5.9 Hz, 2 H), 2.06 (quintet, *J* = 6.1 Hz, 2 H), 1.40 (s, 9 H); ¹³C NMR (100 MHz, CDCl₃) δ 165.98, 162.75, 155.71, 153.62, 153.04, 147.15, 135.39, 135.17, 133.86, 133.20, 128.77, 128.66, 128.42, 127.98, 127.83, 127.76, 127.64, 126.79, 125.77, 125.71, 124.20, 124.12, 122.31, 122.06, 120.97, 119.88, 116.52, 106.79, 106.34, 79.47, 67.51, 64.35, 44.34, 38.59, 33.58, 27.86, 26.10, 25.14. HRESI-MS for C₄₀H₄₂ClN₃O₇ + Na, calcd 734.26035, found 734.25755.

N-(4-Chloro-2-hydroxyphenyl)-3-(3-(3-(3-(methoxymethoxy)propoxy)-2-naphthamido)propoxy)-2-naphthamide (8g). Compound 8g (189 mg, 56%) was prepared as a white solid from 5g (153 mg, 0.52 mmol) and 7a (215 mg, 0.52 mmol) following general procedure C. The product was eluted from the column with dichloromethane–ethyl acetate (20:1 to 10:1): mp 186–187 °C. ¹H NMR (400 MHz, CDCl₃) δ 10.72 (s, 1 H), 8.84 (s, 1 H), 8.75 (s, 1 H), 8.70 (t, *J* = 5.8 Hz, 1 H), 8.18 (d, *J* = 8.7 Hz, 1 H), 7.94–7.90 (m, 2 H), 7.73 (d, *J* = 7.8 Hz, 1 H), 7.71 (d, *J* = 7.8 Hz, 1 H), 7.55–7.50 (m, 2 H), 7.43–7.38 (m, 2 H), 7.25 (s, 1 H), 7.19 (s, 1 H), 7.10 (d, *J* = 2.3 Hz, 1 H), 6.89 (dd, *J* = 8.5, 2.2 Hz, 1 H), 4.62 (s, 2 H), 4.38 (t, *J* = 5.3 Hz, 2 H), 4.31 (t, *J* = 5.9 Hz, 2 H), 3.81 (q, *J* = 6.8 Hz, 2 H), 3.74 (t, *J* = 5.6 Hz, 2 H), 3.30 (s, 3 H), 2.40 (quintet, *J* = 5.8 Hz, 2 H), 2.16 (quintet, *J* = 5.8 Hz, 2 H); ¹³C NMR (100 MHz, CDCl₃) δ 166.26, 163.19, 153.86, 153.79, 147.65, 135.85, 135.83, 134.30, 133.86, 129.15, 128.96, 128.51, 128.22, 128.08, 127.04, 126.30, 126.25, 124.76, 124.72, 122.37, 121.47, 120.31, 116.84, 107.37, 107.26, 96.56, 67.62, 66.94, 65.10, 55.32, 38.71, 29.73, 29.32. HRESI-MS for C₃₆H₃₅ClN₂O₇ + Na, calcd 665.20250, found 665.20026.

tert-Butyl (2-((3-((3-((4-Chloro-2-hydroxyphenyl)-carbamoyl)naphthalen-2-yl)oxy)ethyl)carbamoyl)naphthalen-2-yl)oxy)ethyl)carbamate (8h). Compound 8h (85 mg, 42%) was prepared as a white solid from 5h (100 mg, 0.3 mmol) and 7h (118 mg, 0.3 mmol) following general procedure C. The product was eluted from the column with dichloromethane–ethyl acetate (10:1): mp 220–221 °C. ¹H NMR (400 MHz, DMSO-*d*₆) δ 10.88 (s, 1 H), 10.60 (s, 1 H), 8.74 (s, 1 H), 8.67 (t, *J* = 5.8 Hz, 1 H), 8.43 (d, *J* = 9.4 Hz, 1 H), 8.40 (s, 1 H), 8.05 (d, *J* = 8.2 Hz, 1 H), 7.90 (d, *J* = 7.8 Hz, 1 H), 7.89 (d, *J* = 7.9 Hz, 1 H), 7.83 (d, *J* = 8.2 Hz, 1 H), 7.74 (s, 1 H), 7.58 (t, *J* = 7.4 Hz, 1 H), 7.54 (t, *J* = 7.6 Hz, 1 H), 7.46 (s, 1 H), 7.44 (t, *J* = 7.1 Hz, 1 H), 7.40 (t, *J* = 7.4 Hz, 1 H), 7.13 (t, *J* = 5.6 Hz, 1 H), 6.89–6.84 (m, 2 H), 4.54 (t, *J* = 6.4 Hz, 2 H), 4.09 (t, *J* = 5.0 Hz, 2 H), 4.04 (q, *J* = 5.7 Hz, 2 H), 1.25 (s, 9 H), (one CH₂ is hidden in the water peak at 3.35 ppm); ¹³C NMR (100 MHz, DMSO-*d*₆) δ 165.05, 161.98,

155.97, 153.54, 153.11, 147.68, 135.67, 135.15, 133.21, 131.71, 128.92, 128.51, 127.94, 127.71, 127.49, 126.99, 126.43, 126.38, 126.17, 124.76, 124.41, 123.77, 122.36, 120.93, 118.75, 114.20, 108.42, 107.63, 77.91, 68.25, 67.34, 38.31, 28.02. HRESI-MS for C₃₇H₃₆ClN₃O₇ + Na, calcd 692.21340, found 692.21189.

tert-Butyl (3-((3-((3-((4-Chloro-2-hydroxyphenyl)-carbamoyl)naphthalen-2-yl)oxy)ethyl)carbamoyl)naphthalen-2-yl)oxy)propyl)carbamate (8i). Compound 8i (82 mg, 40%) was prepared as a white solid from 5a (104 mg, 0.3 mmol) and 7h (118 mg, 0.3 mmol) following general procedure C. The product was eluted from the column with dichloromethane–ethyl acetate (10:1): mp 139–140 °C. ¹H NMR (400 MHz, DMSO-*d*₆) δ 10.95 (s, 1 H), 10.59 (s, 1 H), 8.75 (s, 1 H), 8.65 (t, *J* = 4.9 Hz, 1 H), 8.47 (d, *J* = 8.5 Hz, 1 H), 8.29 (s, 1 H), 8.05 (d, *J* = 8.5 Hz, 1 H), 7.89 (d, *J* = 8.1 Hz, 1 H), 7.87 (d, *J* = 8.3 Hz, 1 H), 7.81 (d, *J* = 8.2 Hz, 1 H), 7.70 (s, 1 H), 7.59 (t, *J* = 7.2 Hz, 1 H), 7.52 (t, *J* = 7.6 Hz, 1 H), 7.45 (t, *J* = 7.1 Hz, 1 H), 7.41 (s, 1 H), 7.38 (t, *J* = 7.6 Hz, 1 H), 6.93–6.83 (m, 3 H), 4.52 (t, *J* = 5.8 Hz, 2 H), 4.10 (t, *J* = 5.6 Hz, 2 H), 4.05 (q, *J* = 5.2 Hz, 2 H), 3.01 (t, *J* = 6.3 Hz, 2 H), 1.81 (quintet, *J* = 6.2 Hz, 2 H), 1.23 (s, 9 H); ¹³C NMR (100 MHz, DMSO-*d*₆) δ 165.44, 161.97, 155.69, 153.48, 153.19, 147.69, 135.67, 135.04, 133.26, 131.08, 128.93, 128.52, 128.40, 127.82, 127.69, 127.38, 127.00, 126.46, 126.32, 126.20, 124.77, 124.64, 124.28, 122.23, 120.92, 118.80, 114.22, 108.27, 107.30, 77.52, 67.78, 65.76, 38.41, 36.54, 28.67, 28.03. HRESI-MS for C₃₈H₃₈ClN₃O₇ + Na, calcd 706.22905, found 706.22719.

tert-Butyl (2-((3-((3-((4-Chloro-2-hydroxyphenyl)-carbamoyl)naphthalen-2-yl)oxy)propyl)carbamoyl)-naphthalen-2-yl)oxy)ethyl)carbamate (8j). Compound 8j (74 mg, 54%) was prepared as a white solid from 5h (66 mg, 0.2 mmol) and 7a (81 mg, 0.2 mmol) following general procedure C. The product was eluted from the column with dichloromethane–ethyl acetate (10:1): mp 228–229 °C. ¹H NMR (400 MHz, DMSO-*d*₆) δ 10.86 (s, 1 H), 10.56 (s, 1 H), 8.73 (s, 1 H), 8.51 (t, *J* = 5.9 Hz, 1 H), 8.43 (d, *J* = 9.1 Hz, 1 H), 8.30 (s, 1 H), 8.04 (d, *J* = 8.3 Hz, 1 H), 7.90 (d, *J* = 7.4 Hz, 1 H), 7.88 (d, *J* = 7.9 Hz, 1 H), 7.83 (d, *J* = 8.5 Hz, 1 H), 7.62 (s, 1 H), 7.57 (t, *J* = 7.6 Hz, 1 H), 7.52 (t, *J* = 7.6 Hz, 1 H), 7.46 (s, 1 H), 7.44 (t, *J* = 7.2 Hz, 1 H), 7.38 (t, *J* = 7.5 Hz, 1 H), 7.13 (t, *J* = 5.8 Hz, 1 H), 6.94 (d, *J* = 2.3 Hz, 1 H), 6.85 (dd, *J* = 8.5, 1.9 Hz, 1 H), 4.47 (t, *J* = 5.6 Hz, 2 H), 4.11 (t, *J* = 5.1 Hz, 2 H), 3.65 (q, *J* = 6.1 Hz, 2 H), 2.32 (quintet, *J* = 5.6 Hz, 2 H), 1.29 (s, 9 H) (one CH₂ is hidden in the water peak at 3.35 ppm); ¹³C NMR (100 MHz, DMSO-*d*₆) δ 164.87, 162.08, 155.95, 153.68, 153.48, 147.63, 135.68, 134.97, 133.16, 131.26, 128.92, 128.48, 128.41, 127.75, 127.53, 126.91, 126.35, 126.23, 124.73, 124.62, 124.32, 122.35, 120.95, 118.75, 114.19, 107.92, 107.40, 77.88, 68.19, 67.25, 36.36, 28.60, 28.06. HRESI-MS for C₃₈H₃₈ClN₃O₇ + Na, calcd 706.22905, found 706.22788.

Cell Culture. HEK 293T, HFF and A549 cell lines were obtained from American Tissue Culture Collection (ATCC, Manassas, VA). MDA-MB-231, MDA-MB-468, and MCF-7 cell lines were obtained from Developmental Therapeutics Program at the National Cancer Institute (NCI). The cells were maintained in DMEM (Life Technologies, Grand Island, NY) with nonessential amino acids (Life Technologies) and 10% (v/v) HyClone fetal bovine serum (FBS, GE Healthcare Life Science, Logan, UT) at 37 °C with 5% CO₂. HMEC cells were obtained from Lonza (Walkersville, MA) and were cultured in MEGM complete media (Lonza) supplemented with 10 μg/mL penicillin and 10 μg/mL streptomycin (Life Technologies) at 37 °C under 5% CO₂.

Inhibition of CREB-Mediated Gene Transcription. HEK 293T cells in a 10 cm plate were transfected with pCRE-RLuc (6 μg) with Lipofectamine²⁰⁰⁰ (Life Technologies) following the manufacturer's instructions. Three hours after transfection, the cells were collected and replated into 96-well plates at ~10 000 cells/well. The cells were allowed to attach to the bottom of the plates overnight. The cells were then treated with different concentrations of different compounds for 30 min, when forskolin (10 μM) was added to each well. The cells were incubated for further 5 h before cell lysis using 1× 30 μL *Renilla* luciferase lysis buffer (Promega, Madison, WI). An amount of 5 μL of the lysate was combined with 30 μL of benzyl-coelenterazine (Nanolight, Pinetop, AZ) solution in PBS (pH 7.4, 10 μg/mL). The

protein concentration in each well was determined by Dye Reagent Concentrate (Bio-Rad, Hercules, CA). The *Renilla* luciferase activity was normalized to protein content in each well and expressed as relative luciferase unit/ μg protein (RLU/ μg protein). The IC_{50} was derived from nonlinear regression analysis of the RLU/ μg protein–concentration curve in Prism 5.0 (La Jolla, CA).

Cell Growth Inhibition Assay. The growth inhibition of different cell types was assessed by MTT assay using MTT reagent (Sigma, St. Louis, MO). Briefly, the cells were plated into 96-well plates and the cells were allowed to attach to the bottom of the plates overnight. Then the cells were treated with different concentrations of different drugs for 72 h. The media were removed, and MTT reagent in complete tissue culture media (0.5 mg/mL) was added to each well and incubated at 37 °C for 3 h. The incubation media were removed and 100 μL of DMSO was added to each well. The absorbance of the formed purple formazan solution was read at 570 nm using Packard Fusion plate reader. The percent of growth is defined as $100 \times (A_{\text{treated}} - A_{\text{initial}})/(A_{\text{control}} - A_{\text{initial}})$, where A_{treated} represents absorbance in wells treated with a compound, A_{initial} represents the absorbance at time 0, and A_{control} denotes media-treated cells. The GI_{50} was derived from nonlinear regression analysis of the percent of growth–concentration curve in Prism 5.0.

qRT-PCR. The qRT-PCR assay was carried out essentially in the same way as described before.¹⁷ Briefly, HEK 293T cells were treated with different compounds for 1 h followed by treatment with DMSO or forskolin (10 μM) for 45 min. Then total RNA was isolated and treated with DNase I using NucleoSpin RNA kit (Clontech). The first-strand cDNA was synthesized using SuperScript III First-Strand Synthesis System for RT-PCR (Invitrogen). Quantitative real-time PCR was performed on QuantStudio 7 Flex using SYBR Advantage qPCR Premix (Clontech). The $2^{-\Delta\Delta\text{CT}}$ method was used to analyze the relative changes in gene expression^{16,40} with hypoxanthine phosphoribosyltransferase 1 (*HPRT*) as the reference gene. The primers used were the same as before.¹⁷

In Vivo Xenograft Study. All the procedures for animal handling, care, and the treatment in this study were performed according to the guidelines approved by the Institutional Animal Care and Use Committee (IACUC) of Oregon Health & Science University following the guidelines of the Association for Assessment and Accreditation of Laboratory Animal Care (AAALAC). Each 6- to 8-week old BALB/c nude mouse (Charles River Laboratories) was inoculated subcutaneously at the right flank with MDA-MB-468 cells (5×10^6) in 0.1 mL of HBSS with Matrigel (1:1) for tumor development. When the tumor volume reached approximately 100 mm^3 , the mice were randomized to be treated with either vehicle or **3i** at 10 mg/kg. **3i** was dissolved in 1% *N*-methylpyrrolidone (NMP), 5% Tween-80 in H_2O . The dosing solution was prepared weekly. The mice were treated once a day for 5 consecutive days a week, and the treatment lasted for 5 weeks. During the treatment, the tumor size and body weight were measured 2–3 times a week. The tumors were measured in two dimensions using a digital caliper, and the volume was expressed in mm^3 using the formula $V = 0.5ab^2$, where a and b represent the long and short diameters of the tumor, respectively. The tumor volume was normalized to the initial tumor volume at the time of the first treatment. Student *t*-test was used for statistical analysis.

Molecular Modeling. All the molecular modeling studies were conducted in Schrodinger Small Molecule Drug Discovery Suite (Portland, OR). All the structures were first optimized using MacroModel with MMFFs force field in the absence of any solvent. The charges were from the force field. Powell–Reeves conjugate gradient (PRCG) minimization algorithm was used, and all minimizations were converged to 0.05 $\text{kJ mol}^{-1} \text{\AA}^{-1}$. To identify the global conformational minimum for each compound, the minimized structure was subjected to a conformational search by rotating all the rotatable bonds in each structure. MMFFs force field was used. The global energy minimum was taken for cLogP and PSA calculation using QikProp module.

■ ASSOCIATED CONTENT

■ Supporting Information

Additional supplemental figures, experimental procedures, NMR spectra of **3b–3j**, and a csv file of molecular formula strings. The Supporting Information is available free of charge on the ACS Publications website at DOI: 10.1021/acs.jmedchem.5b00468.

■ AUTHOR INFORMATION

Corresponding Author

*Phone: 1-503-494-4748. Fax: 1-503-494-4352. E-mail: xiaoxi@ohsu.edu.

Author Contributions

[†]F.X. and B.X.L. contributed equally.

Notes

The authors declare no competing financial interest.

■ ACKNOWLEDGMENTS

This work was financially supported by NIH RO1GM087305 (X.X.), RO1CA100855 (R.C.S.), Susan G. Komen KG100458 (X.X.) and DOD BC103625 (R.C.S.). We thank Andrea DeBarber for expert mass spectroscopic analyses. X.X. dedicates this paper to Professor Donglu Bai on the occasion of his 80th birthday.

■ ABBREVIATIONS USED

BOP, (benzotriazol-1-yloxy)tris(dimethylamino)phosphonium hexafluorophosphate; cAMP, cyclic adenosine monophosphate; cLogP, calculated log *P*; CRE, cAMP response element; CREB, cAMP response element binding protein; CBP, CREB binding protein; DEAD, diethyl azodicarboxylate; DIPEA, diisopropylethylamine; HFF, human foreskin fibroblast; HMEC, human mammary epithelial cell; KID, kinase-inducible domain; KIX, KID-interacting domain; MAPK, mitogen-activated protein kinase; MMFF, Merck molecular force field; Nurr1, nuclear receptor related 1 protein; PKA, protein kinase A; PKB, protein kinase B; PP1, protein phosphatase 1; PP2A, protein phosphatase 2A; PSA, polar surface area; PTEN, phosphatase and tensin homolog; qRT-PCR, quantitative reverse transcription polymerase chain reaction; RLuc, renilla luciferase; SD, standard deviation; TEA, triethylamine

■ REFERENCES

- (1) Shaywitz, A. J.; Greenberg, M. E. CREB: A stimulus-induced transcription factor activated by a diverse array of extracellular signals. *Annu. Rev. Biochem.* **1999**, *68*, 821–861.
- (2) Mayr, B.; Montminy, M. Transcriptional regulation by the phosphorylation-dependent factor CREB. *Nat. Rev. Mol. Cell Biol.* **2001**, *2*, 599–609.
- (3) Xiao, X.; Li, B. X.; Mitton, B.; Ikeda, A.; Sakamoto, K. M. Targeting CREB for cancer therapy: friend or foe. *Curr. Cancer Drug Targets* **2010**, *10*, 384–391.
- (4) Radhakrishnan, I.; Perez-Alvarado, G. C.; Parker, D.; Dyson, H. J.; Montminy, M. R.; Wright, P. E. Solution structure of the KIX domain of CBP bound to the transactivation domain of CREB: A model for activator:coactivator interactions. *Cell* **1997**, *91*, 741–752.
- (5) Hagiwara, M.; Alberts, A.; Brindle, P.; Meinkoth, J.; Feramisco, J.; Deng, T.; Karin, M.; Shenolikar, S.; Montminy, M. Transcriptional attenuation following cAMP induction requires PP-1-mediated dephosphorylation of CREB. *Cell* **1992**, *70*, 105–113.
- (6) Wadzinski, B. E.; Wheat, W. H.; Jaspers, S.; Peruski, L. F.; Lickteig, R. L.; Johnson, G. L.; Klemm, D. J. Nuclear-protein phosphatase-2A dephosphorylates protein kinase A phosphorylated

CREB and regulates CREB transcriptional stimulation. *Mol. Cell. Biol.* **1993**, *13*, 2822–2834.

(7) Gu, T.; Zhang, Z.; Wang, J.; Guo, J.; Shen, W. H.; Yin, Y. CREB is a novel nuclear target of PTEN phosphatase. *Cancer Res.* **2011**, *71*, 2821–2825.

(8) Tan, X.; Wang, S.; Zhu, L.; Wu, C.; Yin, B.; Zhao, J.; Yuan, J.; Qiang, B.; Peng, X. cAMP response element-binding protein promotes gliomagenesis by modulating the expression of oncogenic microRNA-23a. *Proc. Natl. Acad. Sci. U.S.A.* **2012**, *109*, 15805–15810.

(9) Rodon, L.; Gonzalez-Junca, A.; Inda, M. D.; Sala-Hojman, A.; Martinez-Saez, E.; Seoane, J. Active CREB1 promotes a malignant TGF- β 2 autocrine loop in glioblastoma. *Cancer Discovery* **2014**, *4*, 1230–1241.

(10) Chhabra, A.; Fernando, H.; Watkins, G.; Mansel, R. E.; Jiang, W. G. Expression of transcription factor CREB1 in human breast cancer and its correlation with prognosis. *Oncol. Rep.* **2007**, *18*, 953–958.

(11) Zhang, S.; Chen, L.; Cui, B.; Chuang, H.-Y.; Yu, J.; Wang-Rodriguez, J.; Tang, L.; Chen, G.; Basak, G. W.; Kipps, T. J. ROR1 is expressed in human breast cancer and associated with enhanced tumor-cell growth. *PLoS One* **2012**, *7*, e31127.

(12) Seo, H. S.; Liu, D. D.; Bekele, B. N.; Kim, M. K.; Pisters, K.; Lippman, S. M.; Wistuba, I. I.; Koo, J. S. Cyclic AMP response element-binding protein overexpression: A feature associated with negative prognosis in never smokers with non-small cell lung cancer. *Cancer Res.* **2008**, *68*, 6065–6073.

(13) Wu, W.; Zhou, H. E.; Huang, W. C.; Iqbal, S.; Habib, F. K.; Sartor, O.; Cvitanovic, L.; Marshall, F. F.; Xu, Z.; Chung, L. W. K. cAMP-responsive element-binding protein regulates vascular endothelial growth factor expression: implication in human prostate cancer bone metastasis. *Oncogene* **2007**, *26*, 5070–5077.

(14) Crans-Vargas, H. N.; Landaw, E. M.; Bhatia, S.; Sandusky, G.; Moore, T. B.; Sakamoto, K. M. Expression of cyclic adenosine monophosphate response-element binding protein in acute leukemia. *Blood* **2002**, *99*, 2617–2619.

(15) Li, B. X.; Xiao, X. Discovery of a small-molecule inhibitor of the KIX-KID interaction. *ChemBioChem* **2009**, *10*, 2721–2724.

(16) Li, B. X.; Yamanaka, K.; Xiao, X. Structure-activity relationship studies of naphthol AS-E and its derivatives as anticancer agents by inhibiting CREB-mediated gene transcription. *Bioorg. Med. Chem.* **2012**, *20*, 6811–6820.

(17) Li, B. X.; Xie, F.; Fan, Q.; Barnhart, K. M.; Moore, C. E.; Rheingold, A. L.; Xiao, X. Novel type of prodrug activation through a long-range O,N-acyl transfer: a case of water-soluble CREB inhibitor. *ACS Med. Chem. Lett.* **2014**, *5*, 1104–1109.

(18) Wu, B.; Basu, S.; Meng, S.; Wang, X.; Hu, M. Regioselective sulfation and glucuronidation of phenolics: insights into the structural basis. *Curr. Drug Metab.* **2011**, *12*, 900–916.

(19) Wu, B.; Kulkarni, K.; Basu, S.; Zhang, S.; Hu, M. First-pass metabolism via UDP-glucuronosyltransferase: a barrier to oral bioavailability of phenolics. *J. Pharm. Sci.* **2011**, *100*, 3655–3681.

(20) Pettersson, M.; Johnson, D. S.; Subramanyam, C.; Bales, K. R.; am Ende, C. W.; Fish, B. A.; Green, M. E.; Kauffman, G. W.; Mullins, P. B.; Navaratnam, T.; Sakya, S. M.; Stiff, C. M.; Tran, T. P.; Xie, L.; Zhang, L.; Pustilnik, L. R.; Vetelino, B. C.; Wood, K. M.; Pozdnyakov, N.; Verhoest, P. R.; O'Donnell, C. J. Design, synthesis, and pharmacological evaluation of a novel series of pyridopyrazine-1,6-dione gamma-secretase modulators. *J. Med. Chem.* **2014**, *57*, 1046–1062.

(21) Mitsunobu, O. The use of diethyl azodicarboxylate and triphenylphosphine in synthesis and transformation of natural products. *Synthesis* **1981**, 1–28.

(22) Kim, S. J.; Baek, H. S.; Rho, H. S.; Kim, D. H.; Chang, I. S.; Lee, O. S.; Shin, H. J. Hydroxybenzamide derivatives, the method for preparing thereof and the cosmetic composition containing the same. WO2007021067A1, 2007

(23) Jiang, M.; Li, B. X.; Xie, F.; Delaney, F.; Xiao, X. Design, synthesis, and biological evaluation of conformationally constrained analogues of naphthol AS-E as inhibitors of CREB-mediated gene transcription. *J. Med. Chem.* **2012**, *55*, 4020–4024.

(24) Xiao, X.; Antony, S.; Kohlhagen, G.; Pommier, Y.; Cushman, M. Design, synthesis, and biological evaluation of cytotoxic 11-amino-alkenylindenoisoquinoline and 11-diaminoalkenylindenoisoquinoline topoisomerase I inhibitors. *Bioorg. Med. Chem.* **2004**, *12*, 5147–5160.

(25) Seamon, K. B.; Padgett, W.; Daly, J. W. Forskolin: unique diterpene activator of adenylate cyclase in membranes and in intact cells. *Proc. Natl. Acad. Sci. U.S.A.* **1981**, *78*, 3363–3367.

(26) Mosmann, T. Rapid colorimetric assay for cellular growth and survival—application to proliferation and cytotoxicity assays. *J. Immunol. Methods* **1983**, *65*, 55–63.

(27) Xie, F.; Li, B. X.; Broussard, C.; Xiao, X. Identification, synthesis and evaluation of substituted benzofurazans as inhibitors of CREB-mediated gene transcription. *Bioorg. Med. Chem. Lett.* **2013**, *23*, 5371–5375.

(28) Lodge, J. M.; Rettenmaier, T. J.; Wells, J. A.; Pomerantz, W. C.; Mapp, A. K. FP tethering: a screening technique to rapidly identify compounds that disrupt protein–protein interactions. *MedChemComm* **2014**, *5*, 370–375.

(29) Moellerling, R. E.; Cravatt, B. F. How chemoproteomics can enable drug discovery and development. *Chem. Biol.* **2012**, *19*, 11–22.

(30) Gleeson, M. P. Generation of a set of simple, interpretable ADMET rules of thumb. *J. Med. Chem.* **2008**, *51*, 817–834.

(31) Yazdani, M.; Glynn, S. L.; Wright, J. L.; Hawi, A. Correlating partitioning and caco-2 cell permeability of structurally diverse small molecular weight compounds. *Pharm. Res.* **1998**, *15*, 1490–1494.

(32) Best, J. L.; Amezcua, C. A.; Mayr, B.; Flechner, L.; Murawsky, C. M.; Emerson, B.; Zor, T.; Gardner, K. H.; Montminy, M. Identification of small-molecule antagonists that inhibit an activator: coactivator interaction. *Proc. Natl. Acad. Sci. U.S.A.* **2004**, *101*, 17622–17627.

(33) Tao, X.; Finkbeiner, S.; Arnold, D. B.; Shaywitz, A. J.; Greenberg, M. E. Ca^{2+} influx regulates BDNF transcription by a CREB family transcription factor-dependent mechanism. *Neuron* **1998**, *20*, 709–726.

(34) Hummler, E.; Cole, T. J.; Blendy, J. A.; Ganss, R.; Aguzzi, A.; Schmid, W.; Beermann, F.; Schutz, G. Targeted mutation of the CREB gene: compensation within the CREB/ATF family of transcription factors. *Proc. Natl. Acad. Sci. U.S.A.* **1994**, *91*, 5647–5651.

(35) Park, Y. G.; Nesterova, M.; Agrawal, S.; Cho-Chung, Y. S. Dual blockade of cyclic AMP response element- (CRE) and AP-1-directed transcription by CRE-transcription factor decoy oligonucleotide. Gene-specific inhibition of tumor growth. *J. Biol. Chem.* **1999**, *274*, 1573–1580.

(36) Chen, J.; Kassenbrock, A.; Li, B. X.; Xiao, X. Discovery of a potent anti-tumor agent through regioselective mono-N-acylation of 7H-pyrrolo[3,2-f]quinazoline-1,3-diamine. *MedChemComm* **2013**, *4*, 1275–1282.

(37) Sakamoto, K. M.; Frank, D. A. CREB in the pathophysiology of cancer: implications for targeting transcription factors for cancer therapy. *Clin. Cancer Res.* **2009**, *15*, 2583–2587.

(38) Konkright, M. D.; Montminy, M. CREB: the undicted cancer co-conspirator. *Trends Cell Biol.* **2005**, *15*, 457–459.

(39) Kang, X.; Lu, Z.; Cui, C.; Deng, M.; Fan, Y.; Dong, B.; Han, X.; Xie, F.; Tyner, J. W.; Coligan, J. E.; Collins, R. H.; Xiao, X.; You, M. J.; Zhang, C. C. The ITIM-containing receptor LAIR1 is essential for acute myeloid leukaemia development. *Nat. Cell Biol.* **2015**, *17*, 665–677.

(40) Pfaffl, M. W. A new mathematical model for relative quantification in real-time RT-PCR. *Nucleic Acids Res.* **2001**, *29*, e45.